ACS Infectious Diseases

Article

pubs.acs.org/journal/aidcbc

Progress against *Escherichia coli* with the Oxazolidinone Class of Antibacterials: Test Case for a General Approach To Improving Whole-Cell Gram-Negative Activity

Khuloud Takrouri,[†] Harold D. Cooper,[‡,Δ] Andrew Spaulding,[§] Paola Zucchi,[⊗] Bilyana Koleva,[§] Dillon C. Cleary,[⊥,Π] Westley Tear,[§] Penny J. Beuning,[§] Elizabeth B. Hirsch,[⊗] and James B. Aggen*[,#]

[†]64 Berkshire Street, Apartment 3, Cambridge, Massachusetts 02141, United States

[‡]9709 Bedder Stone Place, Bristow, Virginia 20136, United States

[§]Department of Chemistry and Chemical Biology, Northeastern University, Boston, Massachusetts 02115, United States

[⊗]Department of Pharmacy and Health Systems Sciences, School of Pharmacy, Northeastern University, Boston, Massachusetts 02115, United States

[⊥]99 Spruce Street, Middleboro, Massachusetts 02346, United States

[#]Revolution Medicines, 700 Saginaw Drive, Redwood City, California 94063, United States

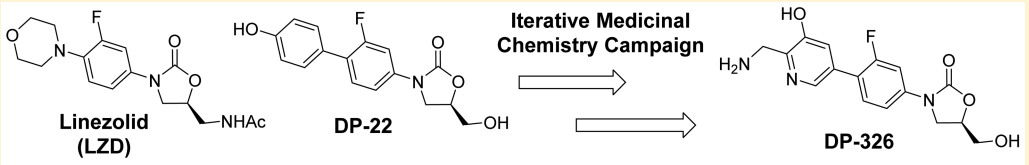

Compound	WT MIC *E.coli*	WT MIC *S.aureus*	Efflux Ratio	Permeability Ratio
LZD	130	3.1	11.6	3.6
DP-22	>256	4	16	>2
DP-326	51	20	1.6	1.6

ABSTRACT: Novel antibacterials with activity against the Gram-negative bacteria associated with nosocomial infections, including *Escherichia coli* and other Enterobacteriaceae, are urgently needed due to the increasing prevalence of multidrug-resistant strains. A major obstacle that has stalled progress on nearly all small-molecule classes with potential for activity against these species has been achieving sufficient whole-cell activity, a difficult challenge due to the formidable outer membrane and efflux barriers intrinsic to these species. Using a set of compound design principles derived from available information relating physicochemical properties to Gram-negative entry or activity, we synthesized and evaluated a focused library of oxazolidinone analogues, a currently narrow spectrum class of antibacterials active only against Gram-positive bacteria. In this series, we have explored the effectiveness for improving Gram-negative activity by identifying and combining beneficial structural modifications in the C-ring region. We have found polar and/or charge-carrying modifications that, when combined in hybrid C-ring analogues, appear to largely overcome the efflux and/or permeability barriers, resulting in improved Gram-negative activity. In particular, those analogues least effected by efflux and the permeation barrier had significant zwitterionic character.

KEYWORDS: *Gram-negative, outer membrane permeability, oxazolidinones, efflux pump, porins*

Gram-negative bacteria (GNB), which include, for example, the Enterobacteriaceae *Klebsiella*, *Enterobacter*, and *Escherichia coli*, as well as the nonfermenters, such as *Acinetobacter baumannii* and *Pseudomonas aeruginosa* and other less common species, are responsible for many serious infections, such as pneumonias, bloodstream infections, wound or surgical site infections, complicated urinary tract infections, and meningitis in healthcare settings.[1] In recent years there has been an alarming rise in multidrug resistance (MDR) across many species of GNB, and strains resistant to most available antibiotics are encountered with increasing regularity.[2]

The effect of this growing problem of antimicrobial-resistant infections on human health was recently quantified in a 2013 report from the Centers for Disease Control and Prevention (CDC).[3] According to this report, 2 million Americans become infected with resistant bacteria each year, 23,000 of whom die as a direct result of these infections. Furthermore, MDR GNB were identified specifically as among the most urgent threats. The impact of this problem is intensified by a lack of new

Received: January 5, 2016
Published: April 14, 2016

DOI: 10.1021/acsinfecdis.6b00003
ACS Infect. Dis. 2016, 2, 405−426

antibacterial drugs in clinical development with GNB activity.[4,5] We believe one of the main obstacles leading to a lack of new agents in development is the lack of published literature describing a rational and reliable approach for evolving early hit compounds into lead compounds with potent whole-cell activity against these pathogens.[6]

GNB are more challenging to target than Gram-positive bacteria (GPB) due to their unique outer membrane (OM) and its associated proteins exterior to their cytoplasmic membrane.[7] The OM acts as a potent barrier to entry of typical drug-like molecules (Figure 1) due to the multiplicative action of three

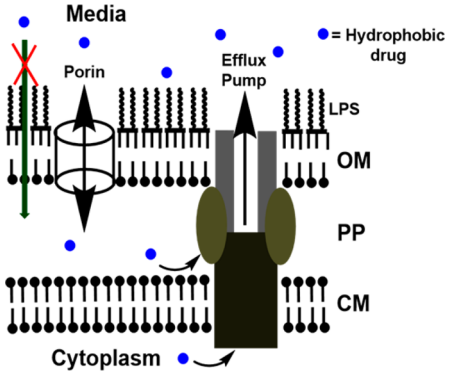

Figure 1. Diagram representing the GNB (*E. coli*) cell envelope. OM, outer membrane; CM, cytoplasmic membrane; PP, periplasm; efflux pump, multisubunit system consisting of TolC, AcrA, and AcrB; LPS, lipopolysaccharide outer membrane component.

components: (i) the outer leaflet, composed of lipopolysaccharide (LPS), which inhibits passive diffusion; (ii) the channel proteins called porins that limit the size and properties of solutes that pass through the OM to the periplasm; and (iii) the efflux pumps that actively transport compounds out of the cytoplasmic membrane and periplasmic space to the cell exterior. The combined effect of these barriers can lead to significantly lower antibacterial activity against common GNB, such as *E. coli*, compared to GPB with agents having potential for broad-spectrum activity; indeed, in our own experiences we have seen the combined impact of these barriers on antibacterial activity in a series of related analogues range from 2- to >256-fold. Unquestionably, the availability of a compound design strategy that reliably enabled medicinal chemists to minimize the impact of these barriers would greatly facilitate the discovery of new antibacterial drugs, but currently such a strategy has not been described in the literature.

In hopes of developing a compound design strategy enabling reliable minimization of the liability of an antibacterial scaffold to the OM barriers, we gleaned the literature for guidance. Available but fragmentary literature data gathered on solutes and antibiotics active against GNB indicate that certain structural properties are key factors influencing how readily compounds pass through the outer barrier.[8−11] Guidelines deduced from these data signal that to be active against GNB, antibacterial compounds should have, in addition to potent target activity, a (i) low molecular weight (MW) (preferably <400), (ii) relatively high polarity (clogD < 1), and (iii) charged character with bias to zwitterionic character at physiological pH. The broad-spectrum orally active fluoroquinolones (FQs; e.g., ciprofloxacin) follow and support these guidelines,[12] despite the fact that they have lost a great deal of their usefulness due to widespread resistance. Additionally, recent retrospective analyses support the view that these physicochemical criteria are important, albeit not sufficient, for GNB activity.[13,14]

We reasoned that by applying the properties above as guidelines for our analogue design strategy we could significantly reduce the combined impact of the OM barriers on a small-molecule antibacterial scaffold. We further reasoned that minimizing the impact of the OM barriers would result in improved GNB whole-cell activity, provided these analogues maintained potent inhibitory activity against their molecular target. This is a target-independent approach with potential for broad application to existing and novel classes of antibiotics currently lacking Gram-negative activity. We have not found reported literature describing attempts of applying this systematic approach for improvement of GNB activity.

Armed with our strategy for minimizing the liability toward the OM barriers by systematic modifications following our guidelines, we needed only to settle on a highly suitable scaffold for our test case. The oxazolidinone family of Gram-positive agents represented an attractive class to start with, as it holds potential as a source for broad-spectrum orally active agents. A great deal of guidance is available to facilitate our efforts on this scaffold, including a significant amount of published structure−activity relationship (SAR) data relating to antibacterial activity,[15−18] available guidance for preclinical evaluation and derisking of novel compounds relating to both the pharmacokinetic/pharmacodynamic (PK/PD) parameters predictive of clinical success for the class,[19,20] and scaffold-associated dose-limiting toxicities.[21−23]

The first successful example in this class, linezolid (Zyvox; Figure 2), is FDA approved for serious infections, including

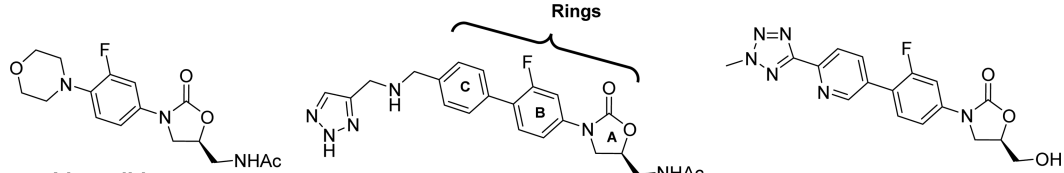

Linezolid
MW = 337.35
clogD$_{7.4}$ = 0.64
No charge character
MRSA MIC$_{90}$ = 4
H. influenzae MIC$_{90}$ = 16

Radezolid
MW = 438.46
clogD$_{7.4}$ = 1.51
Single charge character
MRSA MIC$_{90}$ = 4
H. influenzae MIC$_{90}$ = 1

Tedizolid (Torezolid; TR-700)
MW = 370.34
clogD$_{7.4}$ = 2.12
No charge character
MRSA MIC$_{90}$ = 1
H. influenzae MIC$_{90}$ = 16

Figure 2. Structures of three leading oxazolidinones and some of their properties calculated with ChemAxon. MIC$_{90}$ data are from published papers.[20,33]

DOI: 10.1021/acsinfecdis.6b00003
ACS Infect. Dis. 2016, 2, 405−426

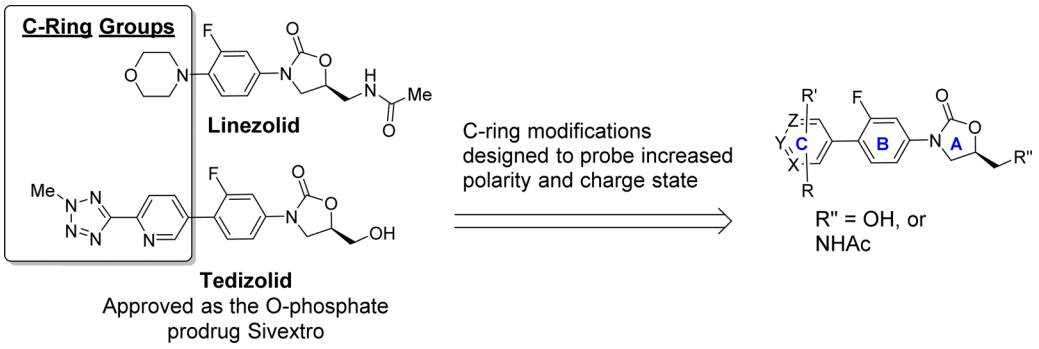

Figure 3. Rational design of Gram-negative penetrating oxazolidinone derivatives.

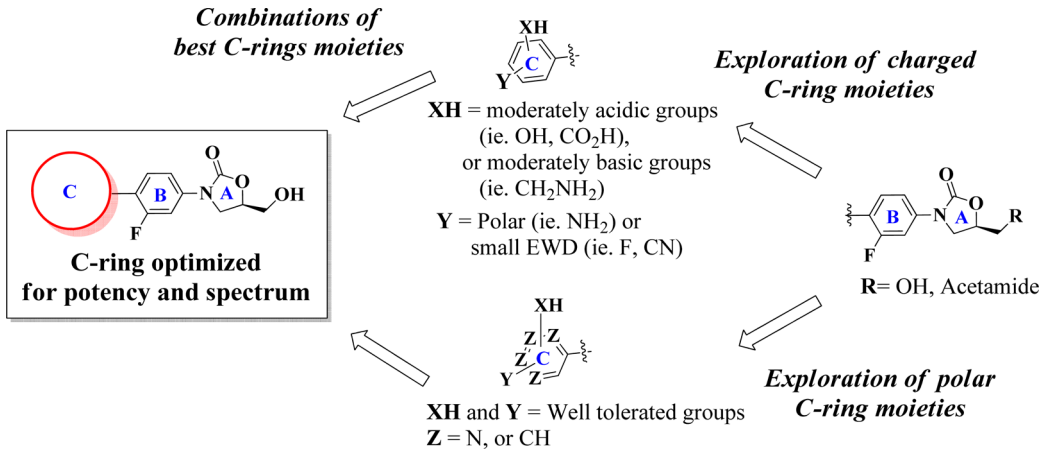

Figure 4. Approach for C-ring optimization.

hospital-acquired pneumonia, and is used for treating infections caused by methicillin-resistant *Staphylococcus aureus* (MRSA).[24] A second member from this class, tedezolid[25] phosphate (Sivextro; parent drug shown in Figure 2), was approved by the FDA in 2014 for use in Gram-positive skin infections. Drugs in this class exert their antibacterial action by binding to a highly conserved region of the 50S subunit of the bacterial ribosome and blocking protein synthesis.[26] A particularly attractive feature of this class is that target-based resistance to linezolid,[27,28] while still rare in Gram-positives[29] and essentially absent in Gram-negatives, can be largely circumvented by known structural modifications.[30] As a testament to their potential for broad-spectrum activity, a newer oxazolidinone currently in clinical development, radezolid (Figure 2), has much improved activity compared to linezolid against *Haemophilus influenzae*.[31] However, so far no member of this drug class with potent activity against the more challenging GNB such as *E. coli*, *P. aeruginosa*, and *A. baumannii* has been reported. Importantly, linezolid demonstrates good potency against *E. coli* when the outer membrane is compromised,[32] thus indicating that an oxazolidinone analogue with the ability to penetrate efficiently into GNB could achieve broader activity.

Herein, we report the results from a rational and systematic medicinal chemistry campaign attempting to minimize the impact of the OM barriers on the oxazolidinone scaffold, thereby achieving equivalent activity against wild-type GNB and GPB. Our approach employed the strategy of designing analogues to have physicochemical properties that conformed to those we deemed vital for GNB activity. Our tactics were to locate these single and multiple polar modifications on the C-ring of the oxazolidinone scaffold, a location known to be tolerant of modification and exposed to solvent when bound to the target site. Each compound prepared was tested against a diagnostic MIC panel of wild-type and OM-compromised *E. coli* strains and a *S. aureus* control strain to determine the impact of structural modifications on OM permeability and efflux liability and to monitor our progress toward bridging the potency gap between the species caused by these barriers. A subset of these analogues was also tested in an in vitro cell-free translation assay to determine their relative inhibitory activity compared to linezolid.

RESULTS AND DISCUSSION

Molecular Design. Oxazolidinone antibacterials, including linezolid and tedizolid, are generally composed of an A-ring (oxazolidinone), a B-ring (phenyl), and a C-ring (varies), with a C-5 side chain unit on the A-ring (Figures 2 and 3). We exploited the available SAR studies incorporating various oxazolidinones and the crystal structure of the first FDA approved oxazolidinone antibiotic, linezolid, bound to the 50S ribosomal subunit[34] to guide our structural design. This information clearly points to the C-ring as the main region in the scaffold appropriate for modifications, given its tolerance for structural variation based on SAR studies and in accord with the reported crystal structure in which this region of linezolid is observed to be exposed to the solvent outside the ribosome binding pocket. Therefore, we focused on this region for exploring the placement of single and multiple polar and charged groups.

Our novel oxazolidinone analogues were designed to incorporate one or more polar and/or charged groups in the C-ring region, to generate a focused library of analogues with

DOI: 10.1021/acsinfecdis.6b00003
ACS Infect. Dis. 2016, 2, 405−426

Scheme 1. Synthetic Route for the General Intermediates Used in the Synthesis of C-Ring-Modified Oxazolidinone Analogues[a]

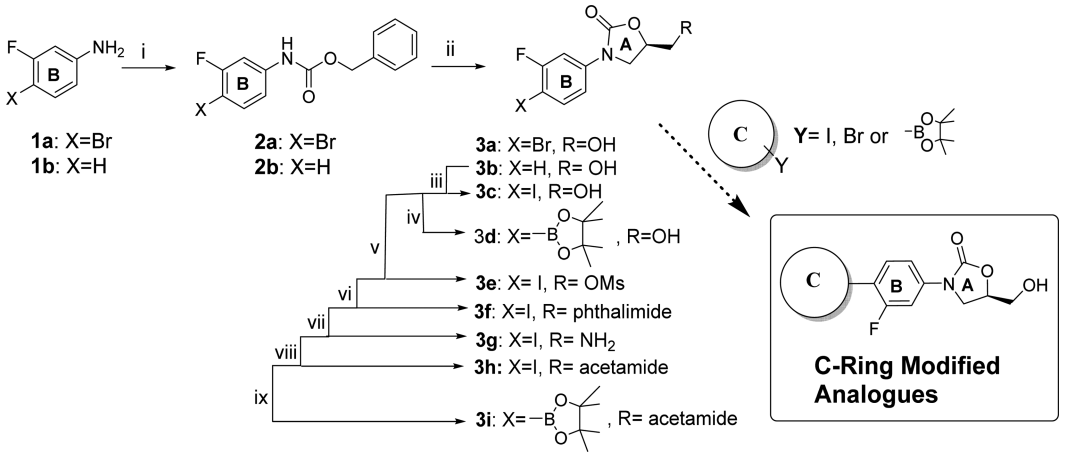

[a]Reagents and reaction conditions: (i) CBz-Cl, K_2CO_3 or $NaHCO_3$, THF, 0 °C to RT, 1−3 h; (ii) *n*-BuLi or LHMDS, (*R*)-(−)-glycidyl butyrate, −78 °C to RT, 12 h; (iii) NIS, TFA, RT, 2 h; (iv) bis(pinacolato)diboron, potassium acetate, $Pd(dppf)_2Cl_2$, DMSO, 80 °C, 12 h; (v) MsCl, TEA, DCM, 0−5 °C, 30 min; (vi) potassium phthalimide, DMF, 70 °C, 4 h; (vii) hydrazine monohydrate, ethanol, reflux, 2 h; (viii) acetic anhydride, TEA, reflux, 1 h; (ix) bis(pinacolato)diboron, potassium acetate, $Pd(dppf)_2Cl_2$, DMSO, 80 °C, 12 h.

optimal physicochemical properties for penetration based on the leading guidance (MW < 400; logD < 1; ionic character at physiologic pH; Figure 3).

Our approach in this study was to first explore the position and character of single ionizable and nonionizable polar groups on the C-ring to identify those that reduce the impact of the OM barriers or those that are best tolerated. After several single modifications inducing a benefit were found, we then turned to bundling these together in hybrid C-ring compounds to gain additive improvements (Figure 4). To facilitate the synthesis effort and keep the MW minimized, we focused on the hydroxymethyl-substituted A-ring series reminiscent of tedizolid and radezolid rather than the *N*-acetylamide A-ring moiety found in linezolid; we confirmed with multiple analogues that no potency difference results in our series from this selection (data not shown).

Synthesis. A general synthetic approach for the assembly of our chiral oxazolidinone ring system, A-ring, with the B-ring intact is shown in Scheme 1. The general intermediates with 4-halo or 4-boronic ester substitution on the B-ring, that is, **3a**, **3c**, **3d**, **3h**, and **3i**, were synthesized in multistep reactions from commercially available anilines using classical methods as described in Scheme 1 and detailed under Methods.

A series of Suzuki coupling reactions was then carried out to produce the C-ring-optimized oxazolidinone analogues. These reactions were carried out using the common intermediates shown in Scheme 1 in either the halide form (i.e., **3a**, **3c**, or **3h**) or boronic ester form (i.e., **3d** or **3i**) together with the intended C-ring that is substituted with boronic acid in the case of using intermediate **3a**, **3c**, or **3h** or with halide in the case of **3d** or **3i**, to form the C-ring/B-ring biaryl system of the planned analogues (see Methods). C-ring moieties were either used as purchased from commercial sources or further synthetically customized either before or after the Suzuki coupling reaction to give the desired functionalities (see Methods).

Determination of the SAR Relating to the OM Barriers. Oxazolidinones typically have good activity against GPB; however, they possess very poor activity against the challenging GNB, such as *E. coli*, due to the combined effect of impaired permeation across the outer membrane and active ejection by efflux pumps.[35] In our hands linezolid, for example, demonstrates a 42-fold potency difference between wild-type *E. coli* and *S. aureus* strains resulting from the combined action of these barriers (Table 1). Penetration of drug into the periplasm is affected by outer membrane permeation and efflux to various degrees, so we felt it critical to determine the SAR for these variables separately. We assessed the impact of efflux on each compound by comparing its MIC for an efflux-competent *E. coli* strain to its MIC for an efflux-deficient mutant of that strain (Δ*acrAB* mutant possessing an intact OM). The ratio of these two MICs is reported in Tables 1−4 as the "efflux ratio". Similarly, the effect of the OM permeation barrier on the antibacterial activity of each compound (permeability ratio, "Perm. ratio") was assessed by comparing its MIC for the parent strain of *E. coli* to its MIC for that strain in the presence of the OM-permeabilizing agent polymyxin-b nonapeptide (PMBN). Compounds were considered improved if they demonstrated reduced efflux and/or permeability ratios and if they demonstrated a reduced potency difference between the *E. coli* and *S. aureus* control strains, relative to linezolid and our starting point (DP-036; Table 1); those compounds that maintained activity against the *S. aureus* strain and demonstrated improved MICs versus the wild-type *E. coli* were of highest interest. All of the *E. coli* strains were from the same genetic background to maintain optimal comparability. A number of compounds in this series had poor solubility, as evident by obvious cloudiness or precipitation formation following dilution from DMSO into media for the MIC testing. In some cases poor solubility prevented us from distinguishing the impact of efflux and the permeation barriers using *E. coli*. However, in these cases we found it useful to consider the difference in activities between the efflux and PMBN-treated *E. coli* strains to the *S. aureus* strain; data we collected with a limited number of compounds (not shown) indicated that the Gram-positive strain was a reasonable surrogate for an *E. coli* with both OM barriers fully compromised (i.e., hyper-permeablized by testing the efflux knockout strain with PMBN present).

Because we made the significant changes from tedizolid of eliminating the tetrazole ring and removing the C-ring pyridyl nitrogen, we considered the unsubstituted C-ring phenyl analogue, **DP-36** (Table 1), as the comparative starting point

DOI: 10.1021/acsinfecdis.6b00003
ACS Infect. Dis. 2016, 2, 405−426

Table 1. MIC Data and Calculated Physicochemical Properties of Mildly Acidic Moieties on C-Ring Oxazolidinone Analogues (Using ChemAxon; clogD at pH 7.4)[a]

C-Ring	Cmpd (n)[b]	Geometric Mean MIC (μg/ml)				Ratios		Physicochemical properties			
		E. coli MG1655 (WT)[c]	*E. coli* +PMBN[d]	*E. coli* Δ*acrAB*[e]	*S. aureus* ATCC 29213[f]	Efflux ratio[g]	Perm. ratio[h]	MW	cpK_a	clogD	% ionized at pH 7.4
	**LZD (40)**	130	36	11	3.1	12	3.6	337.3	>14	0.64	-
	**DP-36**	>64	16	16	1	>8	>8	287.3	>14	2.68	-
	**DP-24**	>256	128	128	32	>4	>4	303.3	>14	2.37	0.95
	**DP-23 (2)**	>256	256	45	5.6	>6	≥2	303.3	>14	2.37	0.45
	**DP-22**	>256	128	16	4	>16	>2	303.3	>14	2.38	0.54
	**DP-35**	>256	16	16	2	>16	>16	321.3	9.06	2.51	2.13
	**DP-43**	>256	32	32	2	>8	>8	321.3	8.27	2.47	11.80
	**DP-4**	>64	>64	64	8	≥2	[#]ND	321.3	8.15	2.45	15.16
	**DP-5 (2)**	>64	16	16	2	>4	>4	321.3	8.17	2.45	14.51
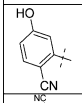	**DP-34**	>256	128	64	32	>4	>2	328.3	7.64	2.04	36.71
	**DP-2**	>512	>512	>512	4	[#]ND	[#]ND	328.3	7.78	2.08	29.29
	**DP-365**	128	32	32	1	4	4	328.3	8.17	2.17	14.64
	**DP-3**	>64	16	16	2	>4	>4	328.3	7.83	2.10	27.03
	**DP-32**	>256	>256	>256	>64	[#]ND	[#]ND	387.3	9.25	3.80	1.40
	**DP-31**	>256	>256	>256	>64	[#]ND	[#]ND	371.3	8.03	3.17	19.00
	**DP-319**	128	8	16	<0.5	8	16	331.3	8.14	2.70	15.38
	**DP-281**	64	64	64	0.5	1	1	350.3	7.73	-2.21	31.83
	**DP-10**	>64	64	16	4	>4	≥2	318.3	10.04	1.55	0.25
	**DP-11**	>64	32	32	4	>2	>2	318.3	9.99	1.55	0.28

DOI: 10.1021/acsinfecdis.6b00003
ACS Infect. Dis. 2016, 2, 405−426

Table 1. continued

[a]MICs reported are mean values from triplicate runs; data were compiled from multiple panel runs. ND, not detected. [b]Number of tests in primary MIC panel if >1. [c]*E. coli* MG1655 (WT), wild-type Gram-negative bacterium *E. coli*. [d]*E. coli* + PMBN, a membrane permeabilized mutant. [e]*E. coli* Δ*acrAB*, an efflux pump deficient strain. [f]*S. aureus* ATCC 29213, Gram-positive bacterium *S. aureus*. [g]Efflux ratio = MIC vs *E. coli*/MIC vs *E. coli* Δ*acrAB*. [h]Permeability ratio = MIC vs *E. coli*/MIC vs *E. coli* + PMBN.

Table 2. MIC Data and Calculated Physicochemical Properties of Mildly Basic Moieties on C-Ring Oxazolidinone Analogues (Using ChemAxon; clogD at pH 7.4)[a]

C-Ring	Cmpd (n)[b]	Geometric Mean MIC (μg/ml)				Ratios		Physicochemical properties			
		E. coli MG1655 (WT)[c]	*E. coli* +PMBN[d]	*E. coli* Δ*acrAB*[e]	*S. aureus* ATCC 29213[f]	Efflux ratio[g]	Perm. ratio[h]	MW	cpK_a	clogD	%ionized at pH 7.4
	**LZD (40)**	130	36	11	3.1	12	3.6	337.3	>14	0.64	-
	**DP-36**	>64	16	16	1	>4	>4	287.3	>14	2.68	-
	**DP-29**	>256	>256	>256	>64	[#]ND	[#]ND	316.3	9.65	-0.38	99.44
	**DP-21**	>256	256	128	32	>4	≥2	316.3	9.42	-0.17	99.05
	**DP-18 (2)**	128	45	16	**2.8**	8	2.8	316.3	9.45	-0.21	99.12
	**DP-368**	256	64	64	4	4	4	344.4	8.82	1.19	96.36
	**DP-315**	>256	64	16	2	>16	>4	342.4	9.55	0.10	99.29
	**DP-343**	>64	8	4	**1**	>16	>8	320.3	1.92	2.00	-
	**DP-367**	>64	32	4	**1**	>16	>4	347.3	13.5	1.28	-
	**DP-380**	128	64	16	4	8	2	346.4	9.11	-0.52	98.10
	**DP-379**	256	64	64	8	4	4	346.4	9.10	-0.51	98.03
	**DP-302**	>256	32	<2	< 0.5	>256	>8	345.3	7.24	1.59	40.80

[a]MICs reported are mean values from triplicate runs; data were compiled from multiple panel runs. ND, not detected. [b]Number of tests in primary MIC panel if >1. [c]*E. coli* MG1655 (WT), wild-type Gram-negative bacterium *E. coli*. [d]*E. coli* + PMBN, a membrane permeabilized mutant. [e]*E. coli* Δ*acrAB*, an efflux pump deficient strain. [f]*S. aureus* ATCC 29213, Gram-positive bacterium *S. aureus*. [g]Efflux ratio = MIC vs *E. coli*/MIC vs *E. coli* Δ*acrAB*. [h]Permeability ratio = MIC vs *E. coli*/MIC vs *E. coli* + PMBN.

for our series. However, due to poor solubility we were unable to test **DP-36** at a high enough concentration to detect its MIC. Therefore, we used linezolid routinely as our positive control for MIC testing because it was soluble enough to determine its MIC against the full set of bacteria.

We began with a systematic exploration of partially charged and polar groups at the different C-ring positions using the hydroxymethyl core scaffold to determine the pattern relating tolerability to their specific placement point and their charge or polarity characteristics, that is, mildly acidic, mildly basic, or polar heterocycles as shown in Tables 1−3. Each of these analogues had the identical A- and B-ring motifs, thereby allowing for best comparability.

DOI: 10.1021/acsinfecdis.6b00003
ACS Infect. Dis. 2016, 2, 405−426

Table 3. MIC Data and Calculated Physicochemical Properties of Heterocyclic Moieties on C-Ring Oxazolidinone Analogues (Using ChemAxon; clogD at pH 7.4)[a]

C-Ring	Cmpd (n)[b]	Geometric Mean MIC (μg/ml)				Ratios		Physicochemical properties			
		E. coli MG1655 (WT)[c]	*E. coli* +PMBN[d]	*E. coli* Δ*acrAB*[e]	*S. aureus* ATCC 29213[f]	Efflux ratio[g]	Perm. ratio[h]	MW	cpK_a	clogD	% ionized at pH 7.4
	**LZD (40)**	130	36	11	3.1	12	3.6	337.3	>14	0.64	-
	**DP-36**	>64	16	16	1	>4	>4	287.3	>14	2.68	-
	**DP-49**	256	16	8	1	32	16	288.3	4.49	1.46	0.12
	**DP-305**	128	64	8	1	16	2	304.3	>14	0.20	-
	**DP-314**	256	64	32	1	8	4	304.3	>14	0.20	-
	**DP-301**	128	32	8	2	16	4	303.3	6.18	1.21	5.63
	**DP-50**	>256	256	64	4	>4	≥2	304.3	6.18	1.76	0.01
	**DP-44 (2)**	**64**	16	5.6	**2**	11	4	303.3	6.20	1.20	5.90
	**DP-42**	>256	256	128	32	>4	≥2	303.3	5.24	1.61	0.69
	**DP-15**	>64	>64	64	8	≥2	[#]ND	304.3	2.98	0.61	-
	**DP-61**	>256	256	256	16	≥2	≥2	317.3	8.46	-0.42	92.03
	**DP-48**	128	64	32	4	4	2	317.3	8.50	-0.46	92.65
	**DP-62**	>256	256	64	8	>4	≥2	335.3	8.09	0.04	83.10

[a]MICs reported are mean values from triplicate runs; data were compiled from multiple panel runs. ND, not detected. [b]Number of tests in primary MIC panel if more than 1. [c]*E. coli* MG1655 (WT), wild-type Gram-negative bacterium *E. coli*. [d]*E. coli* + PMBN, a membrane permeabilized mutant. [e]*E. coli* Δ*acrAB*, an efflux pump deficient strain. [f]*S. aureus* ATCC 29213, Gram-positive bacterium *S. aureus*. [g]Efflux ratio = MIC vs *E. coli*/MIC vs *E. coli* Δ*acrAB*. [h]Permeability ratio = MIC vs *E. coli*/MIC vs *E. coli* + PMBN.

To investigate placement of acidic groups on the C-ring, we first turned to phenols. Phenols are weakly acidic groups that have predictably tunable acidities that rely on the nature and position of substituents on the aryl ring, so they are very useful for exploring the impact of differing pK_a values (i.e., % ionized character at physiological pH) on activity. We also favored

DOI: 10.1021/acsinfecdis.6b00003
ACS Infect. Dis. 2016, 2, 405−426

Table 4. MIC Data and Calculated Physicochemical Properties of C-Ring Hybrid Oxazolidinone Analogues (Charge and Distribution Properties Calculated Using ChemAxon)[a]

C-Ring	Cmpd (n)[b]	Geometric Mean MIC (μg/ml)				Ratios		Physicochemical properties				
		E. coli MG1655 (WT)[c]	*E. coli* +PMBN[d]	*E. coli* Δ*acrAB*[d] [e]	*S. aureus* ATCC 29213[f]	Efflux ratio[g]	Perm. Ratio[h]	MW	cpK_a	clogD	% ionized at pH 7.4	% Zwitterion at pH 7.4
	**LZD (40)**	130	36	11	3.1	12	3.6	337.3	>14	0.64	-	-
	**DP-36**	>64	16	16	1	>4	>4	287.3	>14	2.68	-	-
	**DP-17**	>64	>64	16	4	>4	#ND	332.3	7.98*; 10.29**	-0.06	99.74	20.40
	**DP-19 (4)**	**84**	**32**	**8**	**2.8**	**10.5**	**2.6**	332.3	8.05*; 10.34**	-0.11	99.76	18.13
	**DP-366**	>256	>256	256	64	≥2	#ND	332.3	8.66*; 9.53**	-0.09	97.88	3.08
	**DP-324 (3)**	203	25	10	1.2	20	8.1	333.3	9.65*	1.61	0.56	-
	**DP-325**	**64**	**32**	**64**	**32**	**1**	**2**	350.3	7.86*; 10.18**	0.17	99.69	25.56
	**DP-326 (3)**	**51**	**32**	**32**	**20**	**1.6**	**1.6**	333.3	7.30*; 9.37**	-0.30	98.95	**56.56**
	**DP-300**	>256	128	64	8	>4	>2	329.3	7.21*	1.01	60.96	-
	**DP-63**	>128	16	8	1	>16	>8	328.3	>14	0.88	-	-
	**DP-306**	256	128	32	4	8	2	319.3	9.33*; 6.32**	0.89	8.97	0.23
	**DP-262**	>256	256	32	8	>8	≥2	332.3	8.09**	-0.96	83.03	-
	**DP-16**	>64	>64	>64	>64	#ND	#ND	347.3	1.69*; 5.24**	-1.56	99.91	0.59
	**DP-27**	>256	>256	>256	>256	#ND	#ND	347.3	2.58*; 6.26**	-1.10	99.93	6.64
	**DP-264**	>256	256	128	4	>4	≥2	332.3	7.95*	1.77	21.90	-
	**DP-278**	>256	>256	>256	32	#ND	#ND	346.3	7.90*	1.76	24.00	-
	**DP-279**	>256	>256	256	32	≥2	#ND	347.3	2.72*; 12.75*	-0.81	100.00	-
	**DP-280**	>256	>256	256	32	≥2	#ND	347.3	2.69*; 12.64*	-0.81	100.00	-

DOI: 10.1021/acsinfecdis.6b00003
ACS Infect. Dis. 2016, 2, 405−426

Table 4. continued

C-Ring	Cmpd (n)[b]	Geometric Mean MIC (μg/ml)				Ratios		Physicochemical properties				
		E. coli MG1655 (WT)[c]	*E. coli* +PMBN[d]	*E. coli* Δ*acrAB*[d] [e]	*S. aureus* ATCC 29213[f]	Efflux ratio[g]	Perm. Ratio[h]	MW	cpK_a	clogD	% ionized at pH 7.4	% Zwitterion at pH 7.4
	**DP-304**	>256	>256	64	8	>4	#ND	319.3	9.00*; 10.45*	2.06	2.46	-
	**DP-308**	>256	128	16	4	>16	>2	360.3	8.52*	1.58	7.08	-
	**DP-307**	>256	>256	>256	64	#ND	#ND	360.3	8.47*	1.58	7.85	-
	**DP-321**	**64**	**32**	**64**	**32**	**1**	**2**	361.3	7.96*; 6.10**	1.14	28.18	3.80
	**DP-323**	>256	>256	64	32	>4	#ND	404.4	1.54*; 8.06*; 10.54**	-0.57	99.86	81.88
	**DP-330**	>256	256	64	16	>4	≥2	403.4	8.52*; 7.08**	1.3	38.11	2.62
	**DP-335**	256	64	32	4	8	4	403.4	8.07*; 5.08**; 10.13**	0.17	99.63	17.12
	**DP-336**	>256	>256	>256	>64	#ND	#ND	375.4	8.20*; 7.05**; 10.13**	-0.84	99.79	9.69
	**DP-470**	>256	64	32	2	>8	>4	360.4	8.01*; 9.44**	0.76	97.98	17.60

[a]MICs reported are mean values from triplicate runs; data were compiled from multiple panel runs. ND, not detected. *, pK_a of acidic group present. **, pK_a of protonated basic group present. [b]Number of tests in primary MIC panel if >1. [c]*E. coli* MG1655 (WT), wild-type Gram-negative bacterium *E. coli*. [d]*E. coli* + PMBN, a membrane permeabilized mutant. [e]*E. coli* Δ*acrAB*, an efflux pump deficient strain. [f]*S. aureus* ATCC 29213, Gram-positive bacterium *S. aureus*. [g]Efflux ratio = MIC vs *E. coli*/MIC vs *E. coli* Δ*acrAB*. [h]Permeability ratio = MIC vs *E. coli*/MIC vs *E. coli* + PMBN.

phenols because this moiety is present in numerous antibacterial agents with Gram-negative activity (including the tetracyclines and amoxicillin). The position of the hydroxyl group on the C-ring was found to be important; *meta*- and *para*-phenols, **DP-23** and **DP-22**, respectively, were better tolerated as compared to the *ortho*-phenol, **DP-24** (Table 1). A larger moderately acidic group at the *meta*-position (sulfonamide **DP-344**) was not beneficial. Adding electron-withdrawing groups (EWG) can significantly lower the pK_a values of phenols, whereas electron-releasing groups (ERG) have the opposite effect. To investigate the impact of varying the acidity of the C-ring, phenol analogues with various C-ring EWG groups such as CN, F, CF_3, OCF_3, NO_2, and HCO were synthesized (Table 1). The presence of phenol-acidifying group fluorine (**DP-5**, **DP-35**, and **DP-43**) and CN (**DP-3**, **DP-34**) tended to lower the efflux ratios relative to nonfluorinated comparators **DP-36** and **DP-23**. The specific placement of the phenol-acidifying group fluorine ortho to the phenol was not important as demonstrated by the equal activity of **DP-35** and **DP-5**, indicating that the effect was based on charge character and not other interactions. Interestingly, a stronger and larger EWG at the *para*-position (**DP-281**; NO_2) resulted in a significant increase in the potency difference between the species, despite being apparently unaffected by efflux or the permeation barrier. A more hydrophobic analogue with two fluorines (**DP-316**) demonstrated increased liability toward the OM barriers compared to the monofluoro analogue (**DP-5**). EWD substituents larger than fluorine were not well tolerated at the *ortho*-position, as demonstrated by **DP-34**. On the other hand, adding the ERG NH_2 was reasonably well tolerated, but led to slight increases in the OM barrier effects (**DP-10** and **DP-11**). On the basis of these results, we felt that acidified *meta*-phenols could be relied upon as C-ring substituents to improve permeability and reduce efflux liability to a predictable degree.

To explore mildly basic C-rings, we introduced various amines (**DP-18**, **DP-21**, **DP-29**, **DP-315**, **DP-343**, and **DP-368**), alcohols (**DP-367**), and amino alcohols (**DP-379** and **DP-380**) as seen in Table 2. Of greatest interest in this set was the *para*-methyl amine-substituted moiety, **DP-18**, which maintained baseline activity and had a reduced permeability ratio (Table 2). We next explored placement of a sp2-hybridized (planar) basic group on the C-ring in analogue **DP-302**, which demonstrated improved Gram-positive activity, relative to its comparator **DP-18**, but suffered from a high efflux ratio (Table 2).

Introducing one or more nitrogen atom to the C-ring is calculated to significantly increase overall polarity. To this end we have synthesized and evaluated a number of heterocycles with various substituents on the ring (Table 3). It should be noted that the most efficacious antibiotics of the oxazolidinone class reported to date possess a heterocyclic C-ring. The best analogues in terms of maintaining baseline activity were **DP-44** and **DP-48**. Furthermore, **DP-44** has better activity against *E. coli* than linezolid. It was notable to see that the 3-pyridyl version of **DP-18** (**DP-48**) demonstrated activity similar to it.

On the basis of the results and trends obtained from our first set of compounds, we then set about combining two or more of

DOI: 10.1021/acsinfecdis.6b00003
ACS Infect. Dis. 2016, 2, 405−426

our well-tolerated or beneficial single modifications on the C-ring (Table 4) in hopes of realizing cumulative reductions in the impact of the OM barriers (additive benefits). The C-ring motifs explored via combination in these hybrid analogues included monocharged + neutral polar groups (**DP-324**, **-308**, **-307**, **-278**, and **-264**); multicharged (**DP-304**, **-280**, **-279**, **-323**, **-335**, and **-336**); zwitterionic (**DP-17**, **-19**, **-330**, **-321**, **-325**, **-366**, and **-470**); and polar and charged heterocycles (**DP-300**, **-262**, and **-63**). Additionally, we designed hybrid C-rings that combine all of these variables in zwitterionic heterocycles (**DP-27**, **-16**, **-306**, and **-326**).

Analogues that combined phenol and the aminomethyl substituents were synthesized in compounds **DP-17** and **DP-19** (Table 4). We were encouraged not only to see that the presence of both groups in the C-ring was well tolerated but also to observe an additive benefit relative to the singly modified progenitor compounds. **DP-19** demonstrated lower permeability and efflux ratios, and a correspondingly lower wild-type MIC versus *E. coli*, compared to **DP-23** and **DP-18**. It is important to note that **DP-19** fulfills all three of our criteria based on the leading guidance, that is, MW < 400, logD < 1, and ionic character at physiologic pH with zwitterionic character (see Table 4). Analogues derived from **DP-19** that deviate from one or more of these criteria (such as replacing the methylamine with methyl alcohol, **DP-324**, amide, **DP-264**, and **DP-278**, or reversed amide, **DP-307** and **DP-308**) were less efficient in terms of OM penetration measured by efflux and permeability ratios.

In light of the reduced efflux susceptibility with the more acidic *meta*-phenols, we anticipated that analogues of **DP-19** with phenol-acidifying modifications would lead to even lower efflux and permeability ratios. Thus, we prepared the *ortho*-fluoro version of this compound, **DP-325**. We also anticipated that a *meta*-pyridyl heteroaryl C-ring would have an acidifying effect on the phenol and, thus, prepared the corresponding analogue, **DP-326**. We were pleased to see that both the *ortho*-fluoro analogue **DP-325** and the pyridyl analogue **DP-326** not only followed our prediction but their activity versus *E. coli* was not appreciably affected by either the efflux or permeability barriers (Table 4). In addition, we find it important that these compounds demonstrated nearly identical activity against both species; **DP-326** is 2.5 times more active against *S. aureus* than *E. coli*, whereas linezolid shows a >40-fold difference between the species due to its susceptibility to efflux and the OM permeation barrier. Both **DP-325** and **-326** are calculated to have a higher percent zwitterionic character at physiological pH compared to **DP-19** and most other analogues, and we feel this is an important characteristic allowing them to overcome the OM barriers.

We believe that zwitterionic charge character improves bypass of the OM barriers by optimizing influx through the porins and reducing the rate of efflux, rather than by facilitating other potential routes of entry into the bacteria. Whereas their geometry is suggestive, aminophenols are not iron-chelating siderophore structures, hence they are not expected to make use of the iron uptake mechanisms to gain entry. Although significant zwitterionic character appears important for minimizing the impact of efflux and the permeation barrier, it is not sufficient as evidenced by the higher efflux susceptibility with analogues **DP-27**, **-323**, and **-330**. Thus, as one might anticipate, a certain specificity regarding the placement and nature of the ionizable groups is evident. Furthermore, intensifying charge character in phenyl C-ring analogues that have di- and tricharged moieties on the C-ring was only beneficial in the case of analogues that have zwitterionic character such as **DP-321** and **DP-325**.

However, as is often the case in medicinal chemistry, fixing one problem leads to a new one that must be addressed subsequently in an iterative process. These initial improvements in overcoming the OM barriers introduced a new challenge; our best analogues so far, **DP-325** and **DP-326**, suffered an approximate 8-fold loss in antibacterial potency against the Gram-positive control strain compared to their parent analogues **DP-18**, **-19**, and **-48** and linezolid. A quantitatively similar reduction in inhibitory potency was seen in a cell-free *E. coli* protein synthesis assay indicating that **DP-326** was 4-fold less active than its progenitor **DP-19** and 8-fold less active than linezolid (Table 5). This suggests that the additional structural modifications leading to improved Gram-negative activity and reduced OM and efflux liability of **DP-326**, relative to **DP-19**, were moderately detrimental to its biochemical potency Despite this reduced biochemical activity, the fact that **DP-326** demonstrated a 2.5-fold better MIC value versus *E. coli* compared to linezolid is strongly encouraging, In light of this, our future plans will focus on identifying additional modifications that improve the biochemical potency while maintaining the improvements regarding the OM barriers to further improve the whole-cell GNB activity.

Table 5. Effect of Selected Compounds on Translation of Luciferase

Structure	Compound	TT assay IC_{50} (μg/mL)	Geomean MIC vs. *E. coli* (μg/ml)
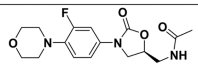	**LZD**	8	130
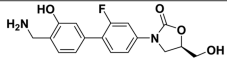	**DP-19**	16	84
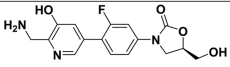	**DP-326**	64	51
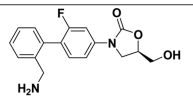	**DP-29**	>128	>256

One intriguing observation we made was regarding the relative activity of analogues in this class against the *S. aureus* and *E. coli* wild-type strains, most notable with those compounds for which multiple repeats of the MIC testing was done. We observed that with those compounds for which the MICs against the whole panel were obtained, the ratio of MIC values from *E. coli* and *S. aureus* (linezolid = 42) was essentially equivalent to the multiple of the efflux and permeability ratios.

In Vitro Transcription/Translation Assay. To determine if our MIC results correlated with activity in inhibiting bacterial protein synthesis, we developed an improved assay to measure inhibition using an *E. coli* in vitro protein synthesis kit with *Gaussia* luciferase expression. After incubation in the presence of compound, the proteins were resolved by SDS-PAGE, the proteins were identified by immunoblotting, and the luciferase expression was quantified using chemiluminescence. Because of the low solubility of **DP-36**, we used linezolid as the control for comparison in these experiments. The results, shown in Table

DOI: 10.1021/acsinfecdis.6b00003
ACS Infect. Dis. 2016, 2, 405−426

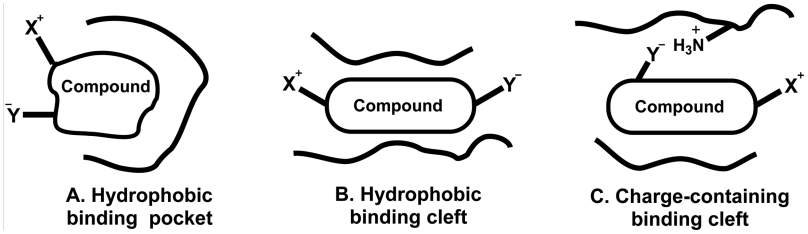

Figure 5. Three possible scenarios that might be encountered with different antibacterial targets and where charge-carrying modifications on the drug compounds might be best tolerated for each.

5, indicate a correlation between potency measured in both the *E. coli* protein synthesis and the *E. coli* MIC assays. This indicates that the reduced antibacterial activity against the WT *E. coli* strain observed with **DP-326** is associated with reduced potency in inhibiting protein synthesis.

CONCLUSIONS

We designed and synthesized a focused set of novel C-ring modified analogues, in the currently narrow-spectrum oxazolidinone class of Gram-positive antibacterial agents, biased to have physicochemical properties correlating with GNB-activity, that is, (i) low MW (preferably <400), (ii) relatively high polarity, and (iii) singly or multiply charged character at physiological pH. On the basis of our present study, polar and/or charge-carrying modifications were identified that reduced susceptibility to the efflux and permeability barriers compared to our starting point, as exemplified by **DP-05** and **DP-18**. When these beneficial modifications were subsequently combined in hybrid C-ring analogues, further reductions in susceptibility to the efflux and permeability barriers was realized as expected from the SAR trends. Several analogues with properties in alignment with those necessary for GNB activity, and calculated to have significant zwitterionic character at pH 7.4, such as **DP-326**, were essentially unaffected by the OM barriers and demonstrated nearly equal antibacterial activity against both the GNB (*E. coli*) and GPB (*S. aureus*) strains tested. Indeed, the antibacterial activity of **DP-326** was elevated <2-fold by both OM barriers, and its resulting MIC against the *E. coli* WT strain was only 2.5 times higher than the MIC against the *S. aureus* strain. In contrast, linezolid and our starting point **DP-36** were >40 times more potent against the *S. aureus* strain compared to *E. coli*, due entirely to the impact of the OM barriers. We believe we have demonstrated that our rational approach, which emphasizes high polarity and zwitterionic character, rapidly led to analogues with minimized liabilities toward the OM barriers in *E. coli*.

However, as is often the case in medicinal chemistry, in learning how to clear the first hurdle of the efflux and permeation barriers, we introduced a new challenge. This new challenge is a moderate 8-fold loss in antibacterial potency we suffered in combining structural modifications to overcome the OM barriers, a loss mirrored by an in vitro protein synthesis inhibition assay results with **DP-326**. Although many unfamiliar with this field may not see the progress, it will be plain to those who have struggled on GNB drug discovery efforts. Moving forward, we are exploring the use of structure-based drug design tactics to find modifications that improve the target inhibition potency. Our expectation is that improving the target inhibitory activity, while maintaining our improvements against the OM barriers, will be a successful path to identifying a broad-spectrum oxazolidinone with promising antibacterial potency.

Although we find our results encouraging, we were unable to arrive at a simplifying "pharmacophore" associated with Gram-negative entry. Indeed, there remains much subtlety that additional research may help unveil. Incorporation of charge-carrying groups to instill zwitterionic character appears important, but determining the optimal identity of the groups and where to place them on each individual scaffold will still require trial and error. However, we offer these suggestions in how our approach may be applied in other situations: (i) Use structural information to guide site-specific modifications. In our case the available crystal structure indicated that the linezolid C-ring protruded out of the binding pocket, thereby providing an attractive location to add polar, charge-carrying moieties. (ii) If structural information is lacking, develop the SAR with charge-carrying groups to identify where they can be placed with minimal loss in activity against hyperpermeable strains and biochemical potency. This is most easily approached by investigating single modifications and combining those that provide even a modest improvement in Gram-negative activity. (iii) Keep in mind that efforts to identify structural modifications that minimize the impact of the OM barriers might initially result in a cost to the biochemical potency, as they appeared to in our case, so an additional round of optimization will likely be necessary to determine how to optimize target potency while maintaining benefits regarding the OM barriers. Three simple scenarios, shown in Figure 5, illustrate how knowledge of the target or SAR might help focus the search for optimal placement of charge-carrying groups. In scenario A, where the target binding pocket is hydrophobic, and therefore not likely to tolerate charged groups, placing modifications such that they sit outside the pocket would be a sensible approach. In scenario B, where the "ends" of an inhibitor are expose to solvent, while the middle region sits in a hydrophobic cleft in the target, investigating the placement of charged groups at either end, as well as bundled on one end, would be sensible. In scenario C, where the target binding cleft or pocket contains a charged group, exploring placement of a modification with the opposite charge to realize a salt bridge would be sensible.

To conclude, these findings are encouraging, important, and exploitable because they resemble a solid base and starting point for additional efforts toward discovering GNB active oxazolidinone antibiotics. Also, these findings strongly support our hypothesis that by applying the compound properties associated with Gram-negative activity into the structural design of the antibiotic, we can build effective Gram-negative whole-cell activity into a scaffold currently lacking it.

METHODS

Chemistry. Experimental procedures and spectral characterization on intermediates in Scheme 1 are described below. All

DOI: 10.1021/acsinfecdis.6b00003
ACS Infect. Dis. 2016, 2, 405−426

reagents and solvents were purchased from commercial sources and used without further purification. Proton, fluorine, and carbon NMR analyses were performed on Varian 400 and 500 MHz spectrometers using DMSO-d_6, acetone-d_6, CD_3OD, D_2O, or $CDCl_3$ as solvent. Chemical shifts (δ) are reported in parts per million relative to TMS or residual solvent peaks. All of the reactions were monitored by LC-MS analysis on a reverse phase column (XBridge BEH C18 column, 130 Å, 4.6 × 100 mm, 3.5 μm particle size), using an Agilent 1100 series LC-MS instrument with the binary system water/acetonitrile containing 0.1% formic acid as eluent. Purifications by flash chromatography were performed on a Teledyne Isco CombiFlash Companion instrument with prepacked Grace silica flash cartridges and were monitored by UV absorbance at 254 and 280 nm. All final compounds were purified using the Dynamax prep HPLC system (XBridge BEH C18 OBD Prep Column, 130 Å, 50 × 250 mm, 10 μm particle size). The purity of all final compounds was determined by analytical HPLC on reverse phase column (XBridge BEH C18 Column, 130 Å, 4.6 × 100 mm, 3.5 μm particle size) using a Hewlett-Packard series 1100 HPLC instrument with the binary system water/acetonitrile containing 0.1% trifluoroacetic acid (TFA) as eluent. On the basis of analytical reversed-phase high-performance liquid chromatography (RP-HPLC) analysis, the purity of all new oxazolidinone analogues reported here exceeded 95%. Their structural identity and integrity were confirmed by LC-MS and ^1H, ^{19}F, and/or ^{13}C NMR.

Biology Assays. *Minimum Inhibitory Concentration (MIC) Testing.* MICs were determined against a set of *E. coli* isolates for Gram-negative activity, and a quality control (ATCC *S. aureus* 29213) strain for Gram-positive activity using the broth microdilution methodology as described by the Clinical and Laboratory Standards Institute.[36] Three strains of *E. coli* were used: (1) a laboratory standard strain (MG1655); (2) MG1655 with the addition of 8 μg/mL polymyxin nonapeptide (PMBN) to permeabilize the outer membrane;[37] and (3) an isogenic derivative of MG1655 (Δ*acrAB*) with the genes encoding the major multidrug resistance efflux system (AcrAB-TolC) deleted.[38] For a subset of compounds, the Δ*acrAB* strain plus 8 μg/mL PMBN was also tested. The ATCC *S. aureus* 29213 is a methicillin-susceptible strain of *S. aureus* and was used in every experiment, along with commercially available linezolid, to ensure that quality control MICs for linezolid against this strain were within range. All MICs were conducted in triplicate in 96-well plates.

In Vitro Transcription/Translation Assay. The expression of *Gaussia* luciferase was evaluated using the PURExpress *In Vitro* Protein Synthesis Kit (New England Biolabs), which uses *E. coli* ribosomes. The *Gaussia* luciferase construct was cloned into a plasmid under T7 control. The 12.5 μL coupled transcription-translation reaction contained 120 ng of plasmid and was supplemented with RNase inhibitor and disulfide enhancer (both from New England Biolabs) in the presence or absence of oxazolidinone test compound. After 1 h of incubation at 37 °C, proteins were resolved by 16% SDS-PAGE and transferred to a PVDF membrane. Anti-Gluc rabbit primary antibody (New England Biolabs) and HRP-conjugated goat anti-rabbit secondary antibody (Thermo Fisher) were used for detection. Chemiluminescence was detected by adding the SuperSignal West Dura Extended Duration Substrate (Thermo Fisher), and the film was processed using a Kodak M35A-M X-OMAT Processor. Band intensities were quantitated using the Image-Quant 1D gel analysis toolbox (GE Lifesciences).

General Procedures for Generation of the Oxazolidinone Derivatives. *General Procedure A.* A solution of **2a** (1 mmol) in anhydrous THF (2 mL) was added to a nitrogen-purged 25 mL flask. Then the desired boronic acid (1.5 mmol) and $PdCl_2(PPh_3)_2$ (0.1 mmol) were added. Once all of the reagents were dissolved in the solution, 2 M aqueous solution of Cs_2CO_3 (3 mmol) was added, and the reaction mixture was placed in a preheated oil bath (65 °C). The mixture was allowed to reflux under vigorous stirring. Once the reaction was deemed complete by TLC and/or LC-MS (2−24 h), it was cooled to room temperature, quenched with DDW (5 mL), and extracted with EtOAc (3 × 5 mL). The combined organic layers were then washed with brine, dried over Na_2SO_4, and concentrated to give a crude product, which was purified by column chromatography on silica gel (6:1 hexane/ethyl acetate).

General Procedure B. A mixture of the desired aryl boronic ester/or acid (1 mmol) and the desired aryl bromide (1 mmol), $Pd(dppf)_2Cl_2$ (0.05 mmol), and K_2CO_3 (4 mmol) in dioxane (3 mL), EtOH (1 mL), and H_2O (1 mL) was added to a nitrogen-purged 25 mL flask. The mixture was heated to 90−95 °C and stirred for 3 h, then cooled to room temperature, filtered, and partially evaporated before 1 M aqueous NaOH solution (10 mL) was added and the mixture was extracted with EtOAc (3 × 10 mL). The organic layers were discarded, and the aqueous layer was acidified by TFA and then extracted with EtOAc (3 × 10 mL). The combined organic layers were then dried over Na_2SO_4 and concentrated under vacuum. The residue was then purified by reversed phase column chromatography on preparative HPLC using a gradient of water/acetonitrile/0.1% TFA. Those fractions containing pure product were pooled and lyophilized to give the pure products.

General Procedure C. The desired aryl bromide (1 mmol) was dissolved in 9:1 dioxane/DDW solvent mixture (2 mL). To this solution was added the corresponding boronic acid/ester (1.2 equiv), $Pd(dppf)Cl_2$ (0.1 equiv), and potassium carbonate (4 equiv). This mixture was then heated to 85−90 °C and stirred for 1−2 h. Upon completion, the reaction was quenched with water (5 mL) and the product extracted with ethyl acetate (3 × 5 mL). The aqueous layer was back-extracted with ethyl acetate (5 mL), and the organic layers were combined and washed with saturated sodium chloride (10 mL), dried over magnesium sulfate, and concentrated to dryness by rotary evaporation. The residue was then purified by reversed phase column chromatography on preparative HPLC using a gradient of water/acetonitrile/0.1% TFA. Those fractions containing pure product were pooled and lyophilized to give the pure products.

General Procedure D. Reduction of nitrile group to methylamino group was achieved as follows: The desired cyano-carrying compounds (1 mmol) was dissolved in anhydrous MeOH (2 mL) and then cooled to 0 °C in an ice bath, and $NiCl_2{\cdot}6H_2O$ (0.08 equiv) was added. Sodium borohydride (6 equiv) was then added in portions, and then the reaction was allowed to warm to room temperature and stirred for 4 h. DDW (5 mL) was then added, and the mixture was extracted in EtOAc (3 × 5 mL). The organic layers were combined, dried over Na_2SO_4, and concentrated under vacuum. The residue was then purified by reversed phase column chromatography on preparative HPLC using a gradient of water/acetonitrile/0.1% TFA. Those fractions containing pure product were pooled and lyophilized to give the pure products.

DOI: 10.1021/acsinfecdis.6b00003
ACS Infect. Dis. 2016, 2, 405−426

(*R*)-3-(2-Fluoro-[1,1′-biphenyl]-4-yl)-5-(hydroxymethyl)oxazolidin-2-one (DP-36). Using general procedure C, bromobenzene and **3d** were employed to afford **DP-36** as a white solid, 84% yield; RP-HPLC (C18), 20−100% (ACN/water/0.1% TFA) in 25 min, t_R = 9.390 min, purity of 99%; ^{1}H NMR (399 MHz, acetone-d_6) δ 7.70 (dt, J = 13.7, 1.9 Hz, 1H), 7.65−7.21 (m, 7H), 4.82 (dddd, J = 9.2, 7.7, 3.7, 1.4 Hz, 1H), 4.22 (td, J = 9.0, 1.5 Hz, 1H), 4.04 (ddd, J = 7.9, 6.1, 1.5 Hz, 1H), 3.91 (ddd, J = 12.3, 3.5, 1.4 Hz, 1H), 3.78 (ddd, J = 12.4, 4.0, 1.4 Hz, 1H), 2.92 (s, 1H); ^{13}C NMR (100 MHz, acetone) δ 158.59, 154.65, 140.29, 140.18, 135.57, 131.03, 130.98, 128.95, 128.92, 128.78, 128.73, 127.70, 123.40, 113.72, 113.69, 105.73, 105.44, 73.66, 62.51, 46.31; ^{19}F NMR (376 MHz, acetone) δ −117.96; LCMS(ESI) $C_{16}H_{14}FNO_3$, $[M + H]^+$, m/z calcd 287.10, found 287.1.

(*R*)-3-(2-Fluoro-2′-hydroxy-[1,1′-biphenyl]-4-yl)-5-(hydroxymethyl)oxazolidin-2-one (DP-24). Using general procedure B, 2-bromophenol and **3d** were employed to afford **DP-24** as a white solid, 51% yield; RP-HPLC (C18) 10−50% (ACN/water/0.1% TFA) in 30 min, t_R = 14.701 min, purity of 97%; ^{1}H NMR (399 MHz, acetone-d_6) δ 8.68 (bs, 1H), 7.64 (dd, J = 12.6, 2.2 Hz, 1H), 7.47−7.31 (m, 2H), 7.26−7.17 (m, 2H), 7.02 (d, J = 8.3 Hz, 1H), 6.91 (t, J = 7.4 Hz, 1H), 4.80 (tt, J = 7.2, 3.3 Hz, 1H), 4.20 (t, J = 8.8 Hz, 1H), 4.03 (dd, J = 8.8, 6.1 Hz, 1H), 3.84 (ddd, J = 48.0, 12.3, 3.8 Hz, 2H); ^{13}C NMR (100 MHz, acetone) δ 158.98, 155.15, 154.83, 139.90, 139.80, 132.41, 131.44, 129.32, 122.79, 121.44, 121.27, 119.58, 116.04, 113.05, 105.38, 105.10, 73.67, 62.53, 46.41; ^{19}F NMR (376 MHz, acetone) δ −113.72; LCMS(ESI) $C_{16}H_{14}FNO_4$, $[M + H]^+$, m/z calcd 304.09, found 304.1.

(*R*)-3-(2-Fluoro-3′-hydroxy-[1,1′-biphenyl]-4-yl)-5-(hydroxymethyl)oxazolidin-2-one (DP-23). Using general procedure B, 3-bromophenol and **3d** were employed to afford **DP-23** as a white solid, 79% yield; RP-HPLC (C18) 10−50% (ACN/water/0.1% TFA) in 30 min, t_R = 13.693 min, purity of 97%; ^{1}H NMR (399 MHz, DMSO-d_6) δ 9.61 (bs, 1H), 7.63−7.29 (m, 3H), 7.24 (t, J = 7.8 Hz, 1H), 6.93 (d, J = 6.6 Hz, 2H), 6.77 (d, J = 8.1 Hz, 1H), 5.25 (m, 1H), 4.73 (m, 1H), 4.11 (t, J = 8.4 Hz, 1H), 3.86 (t, J = 7.3 Hz, 1H), 3.75−3.49 (m, 2H); ^{13}C NMR (100 MHz, DMSO) δ 158.12, 155.04, 140.02, 136.55, 131.42, 130.30, 123.55, 123.28, 119.94, 116.13, 115.31, 114.40, 106.15, 105.86, 74.06, 62.31, 46.64; ^{19}F NMR (376 MHz, DMSO) δ −116.56; LCMS(ESI) $C_{16}H_{14}FNO_4$, $[M + H]^+$, m/z calcd 304.09, found 304.1.

(*R*)-3-(2-Fluoro-4′-hydroxy-[1,1′-biphenyl]-4-yl)-5-(hydroxymethyl)oxazolidin-2-one (DP-22). Using general procedure B, 3-bromophenol and **3d** were employed to afford **DP-22** as a white solid, 54% yield; RP-HPLC (C18) 10−50% (ACN/water/0.1% TFA) in 30 min, t_R = 12.178 min, purity of 99%; ^{1}H NMR (399 MHz, acetone-d_6) δ 8.55 (s, 1H), 7.66 (dt, J = 13.7, 2.6 Hz, 1H), 7.55−7.26 (m, 4H), 7.02−6.79 (m, 2H), 4.86−4.74 (m, 1H), 4.22 (t, J = 8.9 Hz, 1H), 4.03 (dt, J = 7.7, 5.0 Hz, 1H), 3.84 (ddd, J = 50.4, 12.2, 3.9 Hz, 3H), 2.87 (bs, OH); ^{13}C NMR (100 MHz, acetone) δ 158.49, 157.31, 154.62, 139.42, 130.63, 130.57, 130.13, 130.10, 126.63, 115.60, 113.64, 105.75, 105.45, 73.61, 62.51, 46.30; ^{19}F NMR (376 MHz, acetone) δ −118.13; LCMS(ESI) $C_{16}H_{14}FNO_4$, $[M + H]^+$ m/z calcd, 304.09, found 303.8.

(*R*)-3-(2,2′-Difluoro-5′-hydroxy-[1,1′-biphenyl]-4-yl)-5-(hydroxymethyl)oxazolidin-2-one (DP-35). Using general procedure B, 3-bromo-4-fluorophenol and **3d** were employed to afford **DP-35** as a white solid, 69% yield; RP-HPLC (C18) 2−70% (ACN/water/0.1% TFA) in 25 min, t_R = 13.264 min, purity of 97%; ^{1}H NMR (399 MHz, acetone-d_6) δ 7.76−7.51 (m, 1H), 7.42 (tt, J = 11.9, 5.1 Hz, 2H), 7.21−6.95 (m, 1H), 6.93−6.75 (m, 2H), 4.80 (qd, J = 6.3, 3.2 Hz, 1H), 4.21 (tdd, J = 8.6, 7.0, 5.9, 2.6 Hz, 1H), 4.03 (dq, J = 11.8, 5.5, 4.0 Hz, 1H), 3.88 (ddt, J = 9.3, 6.2, 3.4 Hz, 1H), 3.83−3.66 (m, 1H), 2.97 (bs, OH); ^{13}C NMR (100 MHz, acetone) δ 154.62, 153.76, 140.82, 131.81, 127.47, 117.59, 116.37, 116.25, 116.17, 116.12, 113.32, 105.31, 105.02, 73.64, 62.50, 46.30; LCMS(ESI) $C_{16}H_{13}F_2NO_4$, $[M + H]^+$, m/z calcd 322.08, found 322.1.

(*R*)-3-(2,2′-Difluoro-3′-hydroxy-[1,1′-biphenyl]-4-yl)-5-(hydroxymethyl)oxazolidin-2-one (DP-43). Using general procedure B, 3-bromo-2-fluorophenol and **3d** were employed to afford **DP-43** as a white solid, 84% yield; RP-HPLC (C18) 2−50% (ACN/water/0.1% TFA) in 25 min, t_R = 17.177 min, purity of 98%; ^{1}H NMR (399 MHz, DMSO-d_6) δ 9.975 (s, 1H), 7.598 (d, J = 12 Hz, 1H), 7.434 (m, 2H), 7.015 (dt, J = 27.2 Hz, 1H), 6.776 (t, J = 6.8 Hz, 1H), 6.531 (s, 1H), 5.237 (t, J = 5.6 Hz, 1H), 4.729 (m, 1H), 4.118 (t, J = 8 Hz, 1H), 3.862 (t, J = 6.4 Hz, 1H), 3.692−3.529 (m, 2H); LCMS(ESI) $C_{16}H_{13}F_2NO_4$, $[M + H]^+$, m/z calcd 322.08, found 322.1.

(*R*)-3-(2,3′-Difluoro-4′-hydroxy-[1,1′-biphenyl]-4-yl)-5-(hydroxymethyl)oxazolidin-2-one (DP-4). Using general procedure B, 4-bromo-2-fluorophenol and **3d** were employed to afford **DP-4** as a white solid, 78% yield; RP-HPLC (C18) 10−50% (ACN/water/0.1% TFA) in 30 min, t_R = 13.384 min, purity of 96%; ^{1}H NMR (399 MHz, DMSO-d_6) δ 7.57 (dd, J = 13.8, 2.2 Hz, 1H), 7.51 (t, J = 8.9 Hz, 1H), 7.38 (dd, J = 8.6, 2.3 Hz, 1H), 7.31 (dt, J = 12.7, 1.7 Hz, 1H), 7.17 (d, J = 8.4 Hz, 1H), 7.01 (t, J = 8.9 Hz, 1H), 4.71 (ddt, J = 9.4, 6.3, 3.6 Hz, 1H), 4.10 (t, J = 8.9 Hz, 1H), 3.84 (dd, J = 8.9, 6.1 Hz, 1H), 3.61 (ddd, J = 47.9, 12.4, 3.7 Hz, 2H); ^{13}C NMR (100 MHz, DMSO) δ 155.02, 152.66, 150.40, 139.59, 133.60, 131.15, 126.21, 125.53, 118.60, 116.90, 114.42, 106.17, 105.88, 74.04, 62.26, 46.64; ^{19}F NMR (376 MHz, DMSO) δ −116.86, −136.68; LCMS(ESI) $C_{16}H_{13}F_2NO_4$, $[M + H]^+$, m/z calcd 322.08, found 322.0.

(*R*)-3-(2,4′-Difluoro-3′-hydroxy-[1,1′-biphenyl]-4-yl)-5-(hydroxymethyl)oxazolidin-2-one (DP-5). Using general procedure B, 5-bromo-2-fluorophenol and **3d** were employed to afford **DP-5** as a white solid, 88% yield; RP-HPLC (C18) 2−70% (ACN/water/0.1% TFA) in 30 min, t_R = 13.684 min, purity of 97%; ^{1}H NMR (399 MHz, acetone-d_6) δ 8.87 (s, 1H), 7.68 (dd, J = 13.8, 2.2 Hz, 1H), 7.58−7.35 (m, 2H), 7.34−7.11 (m, 2H), 7.02 (ddt, J = 8.3, 4.0, 1.9 Hz, 1H), 4.82 (ddt, J = 9.5, 6.6, 3.6 Hz, 1H), 4.23 (t, J = 8.9 Hz, 1H), 4.04 (dd, J = 8.8, 6.2 Hz, 1H), 3.84 (ddd, J = 50.8, 12.3, 3.7 Hz, 2H); ^{13}C NMR (100 MHz, acetone) δ 154.63, 144.91, 140.27, 140.16, 132.24, 130.91, 130.86, 122.56, 120.58, 118.47, 116.26, 116.08, 113.66, 105.72, 105.42, 73.64, 62.48, 46.29; ^{19}F NMR (376 MHz, acetone) δ −117.78, −140.39; LCMS(ESI) $C_{16}H_{13}F_2NO_4$, $[M + H]^+$, m/z calcd 322.08, found 322.1.

(*R*)-2′-Fluoro-5-hydroxy-4′-(5-(hydroxymethyl)-2-oxo-oxazolidin-3-yl)-[1,1′-biphenyl]-2-carbonitrile (DP-34). Using general procedure B, 2-bromo-4-hydroxybenzonitrile and **3d** were employed to afford **DP-34** as a white solid, 56% yield; RP-HPLC (C18) 2−70% (ACN/water/0.1% TFA) in 30 min, t_R = 12.352 min, purity of 95%; ^{1}H NMR (399 MHz, acetone-d_6) δ 7.82−7.68 (m, 2H), 7.60−7.41 (m, 2H), 7.04 (dd, J = 8.5, 2.5 Hz, 1H), 7.00 (dd, J = 2.4, 0.9 Hz, 1H), 4.84 (ddt, J = 9.6, 6.1, 3.7 Hz, 1H), 4.27 (t, J = 9.0 Hz, 1H), 4.07 (dd, J = 8.8, 6.1 Hz, 1H), 3.97−3.72 (m, 2H); ^{13}C NMR (100 MHz, acetone) δ 161.27, 154.63, 141.32, 135.27, 131.69, 131.65, 118.36, 118.13, 115.89, 113.37, 113.33, 105.37, 105.08,

DOI: 10.1021/acsinfecdis.6b00003
ACS Infect. Dis. 2016, 2, 405−426

103.65, 73.73, 62.54, 46.30; ^{19}F NMR (376 MHz, acetone) δ −115.07; LCMS(ESI) $C_{17}H_{13}FN_2O_4$, $[M + H]^+$, m/z calcd 329.09, found 329.0.

(*R*)-2′-Fluoro-4-hydroxy-4′-(5-(hydroxymethyl)-2-oxooxazolidin-3-yl)-[1,1′-biphenyl]-3-carbonitrile (DP-2). Using general procedure B, 5-bromo-2-hydroxybenzonitrile and **3d** were employed to afford **DP-2** as a tan solid, 88% yield; RP-HPLC (C18) 10−50% (ACN/water/0.1% TFA) in 30 min, t_R = 13.021 min, purity of 95%; ^{1}H NMR (399 MHz, DMSO-d_6) δ 11.33 (bs, OH), 7.73 (s, 1H), 7.68−7.46 (m, 3H), 7.38 (d, J = 8.4 Hz, 1H), 7.07 (d, J = 8.5 Hz, 1H), 4.70 (s, 1H), 4.09 (t, J = 8.7 Hz, 1H), 3.83 (d, J = 7.3 Hz, 1H), 3.65−3.48 (m, 2H); ^{13}C NMR (100 MHz, DMSO) δ 160.43, 158.32, 155.00, 140.05, 135.63, 133.54, 131.20, 126.56, 121.42, 117.45, 117.18, 114.44, 105.82, 99.91, 74.05, 62.25, 46.63; LCMS(ESI) $C_{17}H_{13}FN_2O_4$, $[M + H]^+$, m/z calcd 329.09, found 329.1.

(*R*)-2′-Fluoro-5-hydroxy-4′-(5-(hydroxymethyl)-2-oxooxazolidin-3-yl)-[1,1′-biphenyl]-3-carbonitrile (DP-365). Using general procedure B, 3-bromo-5-hydroxybenzonitrile and **3d** were employed to afford **DP-365** as a creamy solid, 95% yield; RP-HPLC (C18) 2−50% (ACN/water/0.1% TFA) in 30 min, t_R = 17.112 min, purity of 99%; ^{1}H NMR (399 MHz, acetone-d_6) δ 7.72 (dd, J = 13.8, 2.3 Hz, 1H), 7.59 (t, J = 8.7 Hz, 1H), 7.48 (dd, J = 8.6, 2.3 Hz, 1H), 7.41 (q, J = 1.5 Hz, 1H), 7.35 (q, J = 1.8 Hz, 1H), 7.19 (dd, J = 2.4, 1.4 Hz, 1H), 4.84 (ddq, J = 9.3, 7.0, 3.5, 2.8 Hz, 1H), 4.24 (t, J = 9.0 Hz, 1H), 4.06 (dd, J = 8.8, 6.1 Hz, 1H), 3.85 (ddd, J = 51.7, 12.3, 3.6 Hz, 2H); ^{13}C NMR (100 MHz, acetone) δ 161.00, 158.21, 154.63, 141.14, 138.32, 130.97, 123.60, 120.87, 120.83, 118.50, 117.56, 113.82, 113.78, 113.51, 105.72, 105.43, 73.72, 62.48, 46.29; ^{19}F NMR (376 MHz, acetone) δ −117.58; LCMS(ESI) $C_{17}H_{13}FN_2O_4$, $[M + H]^+$, m/z calcd 329.09, found 328.8.

(*R*)-2′-Fluoro-3-hydroxy-4′-(5-(hydroxymethyl)-2-oxooxazolidin-3-yl)-[1,1′-biphenyl]-4-carbonitrile (DP-3). Using general procedure B, 4-bromo-2-hydroxybenzonitrile and **3d** were employed to afford **DP-3** as a tan solid, 62% yield; RP-HPLC (C18) 10−50% (ACN/water/0.1% TFA) in 30 min, t_R = 15.041 min, purity of 96%; ^{1}H NMR (399 MHz, acetone-d_6) δ 9.97 (s, 1H), 7.72 (dd, J = 13.9, 2.2 Hz, 1H), 7.69−7.65 (m, 1H), 7.56 (td, J = 8.8, 2.2 Hz, 1H), 7.48 (dd, J = 8.6, 2.2 Hz, 1H), 7.29 (d, J = 2.1 Hz, 1H), 7.24−7.17 (m, 1H), 4.83 (ddt, J = 9.6, 7.0, 3.4 Hz, 1H), 4.24 (t, J = 8.8 Hz, 1H), 4.06 (dd, J = 8.8, 6.1 Hz, 1H), 3.84 (ddd, J = 52.7, 12.4, 3.4 Hz, 2H); ^{13}C NMR (100 MHz, acetone) δ 161.06, 159.84, 154.59, 141.67, 141.23, 133.58, 130.93, 130.89, 121.54, 120.74, 116.46, 116.42, 113.79, 105.75, 105.46, 99.12, 73.71, 62.46, 46.27; ^{19}F NMR (376 MHz, acetone) δ −116.95; LCMS(ESI) $C_{17}H_{13}FN_2O_4$, $[M + H]^+$, m/z calcd 329.09, found 329.1.

(*R*)-3-(2-Fluoro-4′-hydroxy-3′-(trifluoromethoxy)-[1,1′-biphenyl]-4-yl)-5-(hydroxymethyl)oxazolidin-2-one (DP-32). Using general procedure B, 4-bromo-2-(trifluoromethoxy)phenol and **3d** were employed to afford **DP-32** as a white solid, 88% yield; RP-HPLC (C18) 2−70% (ACN/water/0.1% TFA) in 30 min, t_R = 15.965 min, purity of 99%; ^{1}H NMR (399 MHz, acetone-d_6) δ 7.69 (dd, J = 13.8, 2.3 Hz, 1H), 7.53 (t, J = 8.8 Hz, 1H), 7.49 (dd, J = 2.3, 1.2 Hz, 1H), 7.46 (d, J = 2.1 Hz, 1H), 7.45−7.41 (m, 1H), 7.17 (d, J = 8.5 Hz, 1H), 4.82 (ddt, J = 9.6, 6.2, 3.7 Hz, 1H), 4.23 (t, J = 9.0 Hz, 1H), 4.04 (dd, J = 8.8, 6.2 Hz, 1H), 3.84 (ddd, J = 51.9, 12.4, 3.7 Hz, 2H); ^{13}C NMR (100 MHz, acetone) δ 160.90, 158.47, 154.62, 149.49, 140.00, 136.68, 130.66, 128.92, 128.89, 127.43, 123.44, 118.08, 113.78, 113.74, 105.76, 105.47, 73.65, 62.48, 46.29; ^{19}F NMR (376 MHz, acetone) δ −59.30, −118.22; LCMS(ESI) $C_{17}H_{13}F_4NO_5$, $[M + H]^+$, m/z calcd 388.07, found 388.1.

(*R*)-3-(2-Fluoro-4′-hydroxy-3′-(trifluoromethyl)-[1,1′-biphenyl]-4-yl)-5-(hydroxymethyl)oxazolidin-2-one (DP-31). Using general procedure B, 4-bromo-2-(trifluoromethyl)-phenol and **3d** were employed to afford **DP-31** as a white solid, 76% yield; RP-HPLC (C18) 2−70% (ACN/water/0.1% TFA) in 30 min, t_R = 15.843 min, purity of 100%; ^{1}H NMR (399 MHz, acetone-d_6) δ 9.67 (s, 1H), 7.73 (d, J = 2.1 Hz, 1H), 7.70 (dd, J = 13.8, 2.3 Hz, 1H), 7.66 (dd, J = 8.6, 1.9 Hz, 1H), 7.55 (t, J = 8.8 Hz, 1H), 7.45 (dd, J = 8.6, 2.3 Hz, 1H), 7.19 (d, J = 8.5 Hz, 1H), 4.82 (ddt, J = 9.6, 6.6, 3.7 Hz, 1H), 4.23 (t, J = 8.9 Hz, 1H), 4.05 (dd, J = 8.8, 6.2 Hz, 1H), 3.84 (ddd, J = 51.8, 12.3, 3.7 Hz, 2H); ^{13}C NMR (100 MHz, acetone) δ 158.51, 155.35, 154.63, 140.24, 134.02, 130.71, 130.67, 127.08, 126.65, 122.00, 117.50, 113.79, 113.76, 105.73, 105.44, 94.66, 73.65, 62.48, 46.29; ^{19}F NMR (376 MHz, acetone) δ −63.21, −118.37; LCMS(ESI) $C_{17}H_{13}F_4NO_4$, $[M + H]^+$, m/z calcd 372.08, found 372.1.

(*R*)-2′-Fluoro-3-hydroxy-4′-(5-(hydroxymethyl)-2-oxooxazolidin-3-yl)-[1,1′-biphenyl]-4-carbaldehyde (DP-319). Using general procedure B, 4-bromo-2-hydroxybenzaldehyde and **3d** were employed to afford **DP-319** as a white solid, 85% yield; RP-HPLC (C18) 2−70% (ACN/water/0.1% TFA) in 30 min, t_R = 15.152 min, purity of 100%; ^{1}H NMR (399 MHz, acetone-d_6) δ 7.86 (d, J = 8.0 Hz, 1H), 7.74 (dd, J = 13.9, 2.3 Hz, 1H), 7.64 (t, J = 8.8 Hz, 1H), 7.51 (dd, J = 8.7, 2.3 Hz, 1H), 7.30 (d, J = 8.1 Hz, 1H), 7.18 (s, 1H), 4.84 (ddt, J = 9.5, 6.5, 3.6 Hz, 1H), 4.41 (t, J = 5.8 Hz, 1H), 4.26 (t, J = 9.0 Hz, 1H), 4.13−4.02 (m, 1H), 3.85 (dddd, J = 52.3, 12.2, 6.0, 3.6 Hz, 2H); ^{19}F NMR (376 MHz, acetone) δ −116.54; LCMS(ESI) $C_{17}H_{14}FNO_5$, $[M + H]^+$, m/z calcd 332.09, found 331.9.

(*R*)-3-(2-Fluoro-3′-hydroxy-4′-nitro-[1,1′-biphenyl]-4-yl)-5-(hydroxymethyl)oxazolidin-2-one (DP-281). Using general procedure C, 4-bromo-2-hydroxybenzaldehyde 5-bromo-2-nitrophenol and **3d** were employed to afford **DP-281** as a yellow solid, 40% yield; RP-HPLC (C18) 2−50% (ACN/water/0.1% TFA) in 30 min, t_R = 12.692 min, purity of 95%; ^{1}H NMR (400 MHz, DMSO-d_6) δ 3.59 (m, 1H) 3.70 (m, 1 H) 3.88 (m, 1 H) 4.14 (t, J = 8.79 Hz, 1 H) 4.76 (m, 1H), 5.25 (br s, 9 H), 7.17 (m, 1 H), 7.31 (br s, 1 H), 7.50 (d, J = 8.06, 11 Hz, 1 H), 7.58−7.72 (m, 2 H), 8.00 (d, J = 8.06, 11 Hz, 1 H); LCMS(ESI) $C_{16}H_{13}FN_2O_6$, $[M + H]^+$, m/z calcd 349.08, found 348.8.

(*R*)-3-(4′-Amino-2-fluoro-3′-hydroxy-[1,1′-biphenyl]-4-yl)-5-(hydroxymethyl)oxazolidin-2-one (DP-10). Using general procedure C, 3-amino-5-bromophenol and **3d** were employed to afford **DP-10** as a brown solid, 54% yield; RP-HPLC (C18) 0−30% (ACN/water/0.1% TFA) in 30 min, t_R = 12.384 min, purity of 98%; ^{1}H NMR (399 MHz, methanol-d_4) δ 7.54 (dd, J = 13.4, 2.3 Hz, 1H), 7.41 (t, J = 8.7 Hz, 1H), 7.31 (dd, J = 8.6, 2.3 Hz, 1H), 6.94 (t, J = 1.9 Hz, 1H), 6.88−6.82 (m, 1H), 6.78 (d, J = 8.1 Hz, 1H), 4.80−4.71 (m, 1H), 4.15 (t, J = 8.8 Hz, 1H), 3.99−3.90 (m, 1H), 3.78 (ddd, J = 63.1, 12.5, 3.6 Hz, 2H); ^{19}F NMR (376 MHz, CD_3OD) δ −118.09; LCMS(ESI) $C_{16}H_{15}FN_2O_4$, $[M + H]^+$, m/z calcd 319.10, found 319.1.

(*R*)-3-(3′-Amino-2-fluoro-4′-hydroxy-[1,1′-biphenyl]-4-yl)-5-(hydroxymethyl)oxazolidin-2-one (DP-11). Using general procedure B, 2-amino-4-bromophenol and **3d** were employed to afford **DP-11** as a yellow solid, 44% yield; RP-HPLC (C18) 0−30% (ACN/water/0.1% TFA) in 30 min, t_R =

DOI: 10.1021/acsinfecdis.6b00003
ACS Infect. Dis. 2016, 2, 405−426

11.630 min, purity of 100%; ^{1}H NMR (399 MHz, methanol-d_4) δ 7.62 (d, J = 13.5 Hz, 1H), 7.54−7.43 (m, 3H), 7.37 (d, J = 8.6 Hz, 1H), 7.08 (dd, J = 8.9, 3.6 Hz, 1H), 4.82−4.68 (m, 1H), 4.14 (dd, J = 10.5, 7.0 Hz, 1H), 3.96 (t, J = 7.6 Hz, 1H), 3.78 (ddd, J = 65.6, 12.5, 3.7 Hz, 2H); ^{19}F NMR (376 MHz, CD_3OD) δ −118.46; LCMS(ESI) $C_{16}H_{15}FN_2O_4$, $[M + H]^+$, m/z calcd 319.10, found 319.1.

(*R*)-*N*-(2′,4-Difluoro-4′-(5-(hydroxymethyl)-2-oxo-oxazolidin-3-yl)-[1,1′-biphenyl]-3-yl)methanesulfonamide (DP-342). 5-Bromo-2-fluoroaniline (0.189 g, 1 mmol) was dissolved in anhydrous DCM, and then triethylamine (0.422 mL, 3 mmol) was added. The reaction mixture was then cooled to 0 °C in an ice bath, then methansulfonyl chloride (0.081 mL, 1.05 mmol) was added dropwise, and the reaction mixture was warmed gradually to room temperature and stirred for 1 h to afford *N*-(5-bromo-2-fluorophenyl)methanesulfonamide as confirmed by LC-MS as a white precipitate in quantitative yield, which was filter-dried under vacuum and then used in Suzuki coupling with **3d** without further purification using general procedure C to afford **DP-342** as a white solid, 80% yield.; RP-HPLC (C18) 2−50% (ACN/water/0.1% TFA) in 30 min, t_R = 16.482 min, purity of 100%; ^{1}H NMR (399 MHz, acetone-d_6) δ 8.66 (s, 1H), 8.20 (t, J = 8.6 Hz, 1H), 7.78−7.68 (m, 1H), 7.55−7.32 (m, 4H), 4.83 (t, J = 7.6 Hz, 1H), 4.24 (t, J = 8.9 Hz, 1H), 4.05 (dd, J = 8.8, 6.1 Hz, 1H), 3.84 (ddd, J = 49.7, 12.3, 3.6 Hz, 2H), 2.16 (s, 3H); ^{19}F NMR (376 MHz, acetone) δ −117.82, −126.56; LCMS(ESI) $C_{17}H_{16}F_2N_2O_5S$, $[M + H]^+$, m/z calcd 399.07, found 398.9.

(*R*)-*N*-(2′,4-Difluoro-4′-(5-(hydroxymethyl)-2-oxo-oxazolidin-3-yl)-[1,1′-biphenyl]-3-yl)morpholine-4-sulfonamide (DP-344). 5-Bromo-2-fluoroaniline (0.189 g, 1 mmol) was dissolved in anhydrous DCM, and then triethylamine (0.422 mL, 3 mmol) was added. The reaction mixture was then cooled to 0 °C in an ice bath, then morpholino-4-sulfonyl chloride (0.195 g, 1.05 mmol) was added in portions, and the reaction was warmed gradually to room temperature and stirred for 12 h to afford *N*-(5-bromo-2-fluorophenyl)morpholine-4-sulfonamide as confirmed by LC-MS. The crude was then evaporated to dryness and then used in Suzuki coupling with **3d** without further purification using general procedure C to afford **DP-344** as a brown solid, 80% yield; RP-HPLC (C18) 2−50% (ACN/water/0.1% TFA) in 30 min, t_R = 18.172 min, purity of 100%; ^{1}H NMR (399 MHz, acetone-d_6) δ 8.73 (s, 1H), 7.82 (dt, J = 7.7, 1.8 Hz, 1H), 7.71 (dd, J = 13.8, 2.3 Hz, 1H), 7.57−7.45 (m, 2H), 7.40 (qt, J = 6.7, 2.1 Hz, 1H), 7.32 (dd, J = 10.4, 8.5 Hz, 1H), 4.83 (ddt, J = 9.5, 6.6, 3.4 Hz, 1H), 4.24 (t, J = 9.0 Hz, 1H), 4.05 (dd, J = 8.8, 6.2 Hz, 1H), 3.84 (ddd, J = 51.8, 12.3, 3.6 Hz, 2H), 3.63 (dt, J = 6.9, 2.7 Hz, 5H), 3.24−3.19 (m, 4H); ^{13}C NMR (100 MHz, acetone) δ 155.46, 154.63, 153.01, 130.94, 126.64, 125.26, 116.18, 115.97, 113.82, 105.77, 105.48, 94.66, 73.67, 66.07, 66.01, 62.44, 46.64, 46.29; ^{19}F NMR (376 MHz, acetone) δ −117.79, −128.77; LCMS-(ESI) $C_{20}H_{21}F_2N_3O_6S$, $[M + H]^+$, m/z calcd 470.11, found 469.9.

(*R*)-3-(2′-(Aminomethyl)-2-fluoro-[1,1′-biphenyl]-4-yl)-5-(hydroxymethyl)oxazolidin-2-one (DP-29). Using general procedure C, (2-bromophenyl)methanamine and **3d** were employed to afford **DP-29** as a yellow solid, 58% yield; RP-HPLC (C18) 0−30% (ACN/water/0.1% TFA) in 30 min, t_R = 16.887 min, purity of 95%; ^{1}H NMR (500 MHz, DMSO-d_6) δ 7.54 (dt, J = 12.1, 2.4 Hz, 1H), 7.43 (td, J = 8.3, 6.8 Hz, 1H), 7.35 (ddd, J = 8.3, 2.1, 0.9 Hz, 1H), 6.99−6.91 (m, 1H), 5.24 (s, 1H), 4.72 (ddt, J = 9.6, 6.6, 3.7 Hz, 1H), 4.10 (t, J = 9.0 Hz, 1H), 3.84 (ddd, J = 8.9, 6.2, 0.9 Hz, 1H), 3.63 (ddd, J = 59.1, 12.4, 3.5 Hz, 3H); LCMS(ESI) $C_{17}H_{17}FN_2O_3$, $[M + H]^+$, m/z calcd 317.12, found 317.1.

(*R*)-3-(3′-(Aminomethyl)-2-fluoro-[1,1′-biphenyl]-4-yl)-5-(hydroxymethyl)oxazolidin-2-one (DP-21). Using general procedure C, (3-bromophenyl)methanamine and **3d** were employed to afford **DP-21** as a white solid, 82% yield; RP-HPLC (C18) 2−98% (ACN/water/0.1% TFA) in 15 min, t_R = 4.167 min, purity of 96%; ^{1}H NMR (500 MHz, DMSO-d_6) δ 8.26 (bs, NH_2), 7.77−7.37 (m, 7H), 4.76 (ddt, J = 9.6, 6.4, 3.6 Hz, 1H), 4.23−4.05 (m, 4H), 3.95−3.86 (m, 1H), 3.80−3.53 (m, 2H); LCMS(ESI) $C_{17}H_{17}FN_2O_3$, $[M + H]^+$, m/z calcd 317.12, found 317.1.

(*R*)-3-(4′-(Aminomethyl)-2-fluoro-[1,1′-biphenyl]-4-yl)-5-(hydroxymethyl)oxazolidin-2-one (DP-18). Using general procedure A, *tert*-butyl (4-(4,4,5,5-tetramethyl-1,3,2-dioxaborolan-2-yl)benzyl)carbamate and **3a** were employed to afford *tert*-butyl (*R*)-((2′-fluoro-4′-(5-(hydroxymethyl)-2-oxo-oxazolidin-3-yl)-[1,1′-biphenyl]-4-yl)methyl)carbamate, which was then dissolved in DCM (2 mL), and then TFA (2 mL) was added, and the reaction was stirred at room temperature for 2 h. Then solvent was partially evaporated, water (5 mL) was added, and the product was extracted with ethyl acetate (3 × 5 mL). Then organic layers were combined and partially concentrated before DCM (5 mL) was added. The formed precipitate was filterd and washed with DCM (2× 5 mL) and dried under vacuum to afford **DP-18** as a white solid, 86% yield; RP-HPLC (C18) 0−100% (ACN/water/0.1% TFA) in 25 min, t_R = 9.859 min, purity of 100%; ^{1}H NMR (500 MHz, DMSO-d_6) δ 8.57 (s, 2H), 7.67−7.52 (m, 6H), 7.47 (dt, J = 8.7, 1.9 Hz, 1H), 4.82−4.60 (m, 1H), 4.18−4.11 (m, 1H), 4.06 (d, J = 2.8 Hz, 2H), 3.91 (dd, J = 8.9, 6.1 Hz, 1H), 3.74−3.54 (m, 2H)); LCMS(ESI) $C_{17}H_{17}FN_2O_3$, $[M + H]^+$, m/z calcd 317.12, found 317.2.

(*R*)-3-(4′-((Dimethylamino)methyl)-2-fluoro-[1,1′-biphenyl]-4-yl)-5-(hydroxymethyl)oxazolidin-2-one (DP-368). (*R*)-3-(4′-(Aminomethyl)-2-fluoro-[1,1′-biphenyl]-4-yl)-5-(hydroxymethyl)oxazolidin-2-one, **DP-18** (1 mmol), was dissolved in methanol (1 mL), then formaldehyde (0.70 mmol) was added, and the reaction mixture was stirred at room temperature for 30 min. Sodium cyanoborohydride (2.00 mmol) was then added slowly, and the reaction was stirred at room temperature for 2 h. Then water (5 mL) was added, and the mixture was then extracted with ethyl acetate (3 × 5 mL). Then organic layers were combined, dried over sodium sulfate, and concentrated under vacuum. The resulting crude mixture was dissolved in DMF (1 mL) and purified on a reverse-phase prep-HPLC system (water/acetonitrile/0.1% TFA), and the pure fractions were combined and lyophilized to afford **DP-368** as a light brown solid (97% yield); RP-HPLC (C18) 2−50% (ACN/water/0.1% TFA) in 30 min, t_R = 9.953 min, purity of 97%; ^{1}H NMR (399 MHz, DMSO-d_6) δ 7.68−7.61 (m, 2H), 7.61 (d, J = 2.2 Hz, 1H), 7.60−7.57 (m, 2H), 7.56 (d, J = 2.1 Hz, 1H), 7.50−7.42 (m, 1H), 4.73 (ddt, J = 8.7, 6.2, 2.9 Hz, 1H), 4.31 (s, 2H), 4.21−4.06 (m, 1H), 3.86 (ddd, J = 8.6, 6.1, 2.0 Hz, 1H), 3.76−3.63 (m, 1H), 3.55 (ddd, J = 12.3, 4.1, 1.9 Hz, 1H), 2.74 (s, 6H); LCMS(ESI) $C_{19}H_{21}FN_2O_3$, $[M + H]^+$, m/z calcd 345.15, found 345.8.

(*R*)-3-(4′-(1-Aminocyclopropyl)-2-fluoro-[1,1′-biphenyl]-4-yl)-5-(hydroxymethyl)oxazolidin-2-one (DP-315). Using general procedure C, 4-bromostyrene oxide and **3d** were employed to afford **DP-315** as an off-white solid, 40% yield; RP-HPLC (C18) 2−30% (ACN/water/0.1% TFA) in 30

DOI: 10.1021/acsinfecdis.6b00003
ACS Infect. Dis. 2016, 2, 405−426

min, t_R = 11.601 min, purity of 95%; ^{1}H NMR (400 MHz, DMSO-d_6) δ 1.27 (m, 2H), 1.36 (m, 2 H), 3.59 (m, 1H), 3.69 (m, 1H), 3.89 (m, 1H), 4.13 (t, J = 9.16 Hz, 1H), 4.76 (m, 1H), 5.26 (bs, 1H) 7.43−7.54 (m, 3H), 7.54−7.69 (m, 4H), 8.69 (bs, 2H); LCMS(ESI) $C_{19}H_{19}FN_2O_3$, $[M + H]^+$, m/z calcd 343.14, found 343.2.

(*R*)-3-(3′-Amino-2,4′-difluoro-[1,1′-biphenyl]-4-yl)-5-(hydroxymethyl)oxazolidin-2-one (DP-343). Using general procedure B, 5-bromo-2-fluoroaniline and **3d** were employed to afford **DP-343** as a creamy solid, 95% yield; RP-HPLC (C18) 2−50% (ACN/water/0.1% TFA) in 30 min, t_R = 15.045 min, purity of 95%; ^{1}H NMR (399 MHz, DMSO-d_6) δ 7.57 (dd, J = 13.7, 2.2 Hz, 1H), 7.48−7.35 (m, 2H), 7.06 (dd, J = 11.4, 8.4 Hz, 1H), 6.96 (dt, J = 8.7, 1.9 Hz, 1H), 6.68 (ddt, J = 8.1, 3.9, 1.8 Hz, 1H), 4.71 (ddt, J = 9.4, 6.3, 3.6 Hz, 1H), 4.10 (t, J = 9.0 Hz, 1H), 3.84 (dd, J = 8.9, 6.1 Hz, 1H), 3.61 (ddd, J = 48.4, 12.4, 3.6 Hz, 2H); ^{19}F NMR (376 MHz, DMSO) δ −116.55, −136.23; LCMS(ESI) $C_{16}H_{14}F_2N_2O_3$, $[M + H]^+$, m/z calcd 321.10, found 320.9.

(5*R*)-3-(4′-(1,2-Dihydroxyethyl)-2-fluoro-[1,1′-biphenyl]-4-yl)-5-(hydroxymethyl)oxazolidin-2-one (DP-367). Using general procedure C, 1-bromostyrene oxide and **3d** resulted in a mixture of the epoxide and diol product. **DP-367** was then isolated by preparative HPLC in which residual unopened epoxide was converted to the diol form on the column, off-white, 40% yield; RP-HPLC (C18) 2−30% (ACN/water/0.1% TFA) in 30 min, t_R = 11.766 min, purity of 95%; ^{1}H NMR (400 MHz, DMSO-d_6) δ 3.44 (t, J = 5.86 Hz, 1H), 3.51−3.60 (m, 1H), 3.61−3.69 (m, 1H), 3.87 (d, J = 5.86 Hz, 1H), 4.06−4.15 (m, 1H), 4.51−4.61 (m, 1H), 4.67−4.81 (m, 2H), 5.18−5.35 (m, 3H), 7.35−7.64 (m, 7H); LCMS(ESI) $C_{18}H_{18}FNO_5$, $[M + H]^+$, m/z calcd 348.12, found 347.8.

(5*R*)-3-(4′-(1-Amino-2-hydroxyethyl)-2-fluoro-[1,1′-biphenyl]-4-yl)-5-(hydroxymethyl)oxazolidin-2-one (DP-379). (5*R*)-3-(4′-(1,2-dihydroxyethyl)-2-fluoro-[1,1′-biphenyl]-4-yl)-5-(hydroxymethyl)oxazolidin-2-one, **DP-367** (0.346g, 1 mmol), was dissolved in a mixture of aqueous ammonium hydroxide in dioxane 1:1 (5 mL) and heated at 130 °C in a microwave reactor. This gave a mixture of two isomers, **DP-379** and **DP-380**. Then solvent was evaporated to dryness, and the products were then separated on preparative HPLC. Isomer **DP-379** was obtained as a white solid, 40% yield; RP-HPLC (C18) 2−30% (ACN/water/0.1% TFA) in 30 min, t_R = 17.361 min, purity of 95%; ^{1}H NMR (400 MHz, DMSO-d_6) δ 2.87 (s, 1H), 3.07 (bs, 1H), 3.56 (dd, J = 12.46, 3.66 Hz, 1H), 3.68 (dd, J = 12.09, 3.30 Hz, 1H), 3.87 (dd, J = 8.79 Hz, 1H), 4.05−4.16 (m, 1H), 4.73 (bs, 1H), 4.73 (m, 1H), 4.83 (m, 1H), 6.13 (bs, 1H), 7.38−7.65 (m, 6H), 7.93 (bs, 2H), 8.38 (bs, 1H); LCMS(ESI) $C_{18}H_{19}FN_2O_4$, $[M + H]^+$, m/z calcd 347.13, found 346.8.

(5*R*)-3-(4′-(2-Amino-1-hydroxyethyl)-2-fluoro-[1,1′-biphenyl]-4-yl)-5-(hydroxymethyl)oxazolidin-2-one (DP-380). The second isomer from the synthesis of **DP-379**, that is, **DP-380**, was obtained as a white solid, 40% yield; RP-HPLC (C18) 2−30% (ACN/water/0.1% TFA) in 30 min, t_R = 17.605 min, purity of 95%; LCMS(ESI) $C_{18}H_{19}FN_2O_4$, $[M + H]^+$, m/z calcd 347.13, found 346.8.

(*R*)-2′-Fluoro-*N*′-hydroxy-4′-(5-(hydroxymethyl)-2-oxo-oxazolidin-3-yl)-[1,1′-biphenyl]-4-carboximidamide (DP-302). 4-Bromobenzonitrile (0.182 g, 1 mmol) was added to a nitrogen-purged round-bottom flask along with 50% hydroxylamine hydrochloride in water (1 mmol) and sodium hydroxide (0.400 g, 1 mmol). The solids were then dissolved in ethanol (2 mL), and the reaction mixture was heated to 80 °C and stirred for 2 h. Then solvent was removed under reduced pressure, and the resulting residue was dissolved in EtOAc (5 mL) and then extracted with DDW (3 × 5 mL); the organic layer was dried using Na_2SO_4 and concentrated under vacuum to afford 4-bromo-*N*′-hydroxybenzimidamide as was evident by LC-MS (yield 89%). The product was then used in Suzuki coupling with **3d** without further purification using general procedure B to afford **DP-302** as a light yellow solid, 72% yield; RP-HPLC (C18) 2−50% (ACN/water/0.1% TFA) in 30 min, t_R = 9.713 min, purity of 99%; ^{1}H NMR (399 MHz, acetone-d_6) δ 8.61 (s, 1H), 8.03 (d, J = 8.4 Hz, 1H), 7.96−7.84 (m, 2H), 7.79−7.69 (m, 2H), 7.62 (t, J = 8.8 Hz, 1H), 7.50 (dd, J = 8.6, 2.3 Hz, 1H), 4.83 (m, 1H), 4.25 (t, J = 8.9 Hz, 1H), 4.06 (dd, J = 8.8, 6.2 Hz, 1H), 3.91 (dd, J = 12.3, 3.4 Hz, 1H), 3.78 (dd, J = 12.4, 3.9 Hz, 1H); LCMS(ESI) $C_{17}H_{16}FN_3O_4$, $[M + H]^+$, m/z calcd 346.11, found 345.9.

(*R*)-3-(3-Fluoro-4-(pyridin-4-yl)phenyl)-5-(hydroxymethyl)oxazolidin-2-one (DP-49). Using general procedure C, 4-bromopyridine and **3d** were employed to afford **DP-49** as a light yellow solid, 73% yield; RP-HPLC (C18) 0−50% (ACN/water/0.1% TFA) in 30 min, t_R = 7.882 min, purity of 95%; ^{1}H NMR (500 MHz, DMSO-d_6) δ 8.84 (tq, J = 5.1, 1.8 Hz, 2H), 7.97 (d, J = 11.2 Hz, 2H), 7.89−7.81 (m, 1H), 7.74 (dd, J = 14.2, 2.2 Hz, 1H), 7.58 (dd, J = 8.7, 2.2 Hz, 1H), 4.78 (ddt, J = 9.4, 6.3, 3.5 Hz, 1H), 4.17 (t, J = 9.1 Hz, 1H), 3.92 (dd, J = 9.0, 6.1 Hz, 1H), 3.66 (ddd, J = 62.2, 12.4, 3.5 Hz, 2H); LCMS(ESI) $C_{15}H_{13}FN_2O_3$, $[M + H]^+$, m/z calcd 289.09, found 289.1.

(*R*)-4-(2-Fluoro-4-(5-(hydroxymethyl)-2-oxo-oxazolidin-3-yl)phenyl)pyridine 1-oxide (DP-305).[29] Urea hydrogen peroxide (0.483 g, 5.14 mmol) and potassium carbonate (1.421g, 10.28 mmol) were stirred in anhydrous dioxane (40 mL) for 1 h. Then the mixture was cooled to 0 °C in an ice bath, and then trifluoroacetic anhydride (1.4 mL, 5.14 mmol) was added dropwise. This solution was warmed to room temperature, and **DP-49** (1 mmol) was dissolved in anhydrous dioxane (1 mL) and then added to the reaction mixture. This reaction was heated to 50 °C and stirred for 12 h. The solvent was then removed under vacuum, and the crude product was then dissolved in water and purified by preparative HPLC to afford **DP-305** as an off-white solid, 60% yield; RP-HPLC (C18) 2−30% (ACN/water/0.1% TFA) in 30 min, t_R = 8.187 min, purity of 95%; ^{1}H NMR (400 MHz, DMSO-d_6) δ 3.52−3.63 (dd, J = 12.09, 4.03 Hz, 1H), 3.69 (dd, J = 12.46, 4.03 Hz, 1H), 3.91 (m, 1 H), 4.14 (t, J = 9.16 Hz, 1H), 4.75 (m, 2H), 7.51 (dd, J = 8.06, 2.20 Hz, 1H), 7.68 (m, 2H), 7.72 (m, 2H), 8.33 (d, J = 6.60 Hz, 2H); LCMS(ESI) $C_{15}H_{13}FN_2O_4$, $[M + H]^+$, m/z calcd 305.09, found 304.9.

(*R*)-3-(4-(6-Aminopyridin-3-yl)-3-fluorophenyl)-5-(hydroxymethyl)oxazolidin-2-one (DP-301). Using general procedure C, 5-iodopyridin-2-amine and **3d** were employed to afford **DP-301** as a creamy solid, 80% yield; RP-HPLC (C18) 2−30% (ACN/water/0.1% TFA) in 30 min, t_R = 11.601 min, purity of 97%; ^{1}H NMR (399 MHz, DMSO-d_6) δ 8.29 (s, 2H), 8.08 (s, 1H), 7.79−7.71 (m, 1H), 7.61−7.54 (m, 1H), 7.51 (td, J = 8.8, 1.9 Hz, 1H), 7.38 (dt, J = 8.8, 2.0 Hz, 1H), 6.72 (d, J = 8.8 Hz, 1H), 4.69 (dt, J = 12.1, 4.4 Hz, 1H), 4.13−4.03 (m, 1H), 3.87−3.78 (m, 1H), 3.65 (dd, J = 12.2, 3.0 Hz, 1H), 3.57−3.48 (m, 1H); ^{19}F NMR (376 MHz, DMSO) δ −116.76); LCMS(ESI) $C_{15}H_{14}FN_3O_3$, $[M + H]^+$, m/z calcd 304.10, found 303.9.

DOI: 10.1021/acsinfecdis.6b00003
ACS Infect. Dis. 2016, 2, 405−426

(*R*)-3-(3-Fluoro-4-(2-hydroxypyridin-4-yl)phenyl)-5-(hydroxymethyl)oxazolidin-2-one (DP-50). Using general procedure B, 4-bromopyridin-2-ol and **3d** were employed to afford **DP-50** as a yellow solid; RP-HPLC (C18) 2−60% (ACN/water/0.1% TFA) in 15 min, t_R = 4.600 min, purity of 95%; ^{1}H NMR (500 MHz, DMSO-d_6) δ 7.70−7.60 (m, 2H), 7.54−7.42 (m, 2H), 6.49 (d, J = 1.6 Hz, 1H), 6.39 (dt, J = 6.9, 1.7 Hz, 1H), 4.76 (ddt, J = 9.4, 6.3, 3.5 Hz, 1H), 4.14 (t, J = 9.0 Hz, 1H), 3.88 (dd, J = 8.9, 6.0 Hz, 1H), 3.79−3.66 (m, 9H), 3.58 (dd, J = 12.4, 4.0 Hz, 1H); LCMS(ESI) $C_{15}H_{13}FN_2O_4$, $[M + H]^+$, m/z calcd 305.09, found 305.1.

(*R*)-3-(4-(2-Aminopyridin-4-yl)-3-fluorophenyl)-5-(hydroxymethyl)oxazolidin-2-one (DP-44). Using general procedure B, 4-bromopyridin-2-amine and **3d** were employed to afford **DP-44** as an off-white solid; RP-HPLC (C18) 0−30% (ACN/water/0.1% TFA) in 30 min, t_R = 13839 min, purity of 98%; ^{1}H NMR (500 MHz, DMSO-d_6) δ 8.03 (d, J = 6.4 Hz, 2H), 7.85−7.67 (m, 2H), 7.56 (dd, J = 8.7, 2.2 Hz, 1H), 7.16 (s, 1H), 7.07 (d, J = 6.7 Hz, 1H), 4.78 (ddt, J = 9.3, 6.2, 3.5 Hz, 1H), 4.16 (t, J = 9.1 Hz, 1H), 3.91 (dd, J = 9.0, 6.0 Hz, 1H), 3.65 (ddd, J = 62.9, 12.4, 3.5 Hz, 2H); LCMS(ESI) $C_{15}H_{14}FN_3O_3$, $[M + H]^+$, m/z calcd 304.10, found 304.1.

(*R*)-3-(4-(6-Aminopyridin-2-yl)-3-fluorophenyl)-5-(hydroxymethyl)oxazolidin-2-one (DP-42). Using general procedure C, 6-bromopyridin-2-amine and **3d** were employed to afford **DP-42** as a white solid, 74% yield; RP-HPLC (C18) 2−30% (ACN/water/0.1% TFA) in 30 min, t_R = 11.601 min, purity of 90%; ^{1}H NMR (500 MHz, DMSO-d_6) δ 7.88 (t, J = 8.1 Hz, 1H), 7.72 (dd, J = 13.8, 2.2 Hz, 1H), 7.54 (dd, J = 8.8, 2.3 Hz, 1H), 7.03 (d, J = 7.3 Hz, 1H), 6.89 (d, J = 8.8 Hz, 1H), 4.78 (ddt, J = 9.6, 6.7, 3.5 Hz, 1H), 4.16 (t, J = 9.0 Hz, 1H), 3.91 (dd, J = 8.9, 6.0 Hz, 1H), 3.65 (ddd, J = 61.5, 12.4, 3.6 Hz, 2H); LCMS(ESI) $C_{15}H_{14}FN_3O_3$, $[M + H]^+$, m/z calcd 304.10, found 304.1.

(*R*)-3-(4-(2-Aminopyrimidin-5-yl)-3-fluorophenyl)-5-(hydroxymethyl)oxazolidin-2-one (DP-15). Using general procedure A, (2-aminopyrimidin-5-yl)boronic acid and **3a** were employed to afford **DP-15** as a white solid; RP-HPLC (C18) 0−30% (ACN/water/0.1% TFA) in 30 min, t_R = 20.879 min, purity of 98%; LCMS(ESI) $C_{14}H_{13}FN_4O_3$, $[M + H]^+$, m/z calcd 305.10, found 305.2.

(*R*)-3-(4-(2-(Aminomethyl)pyridin-4-yl)-3-fluorophenyl)-5-(hydroxymethyl)oxazolidin-2-one (DP-61). Using general procedure C, (4-bromopicolinonitrile and **3d** were employed to afford (*R*)-4-(2-fluoro-4-(5-(hydroxymethyl)-2-oxo-oxazolidin-3-yl)phenyl)picolinonitrile, which was then reduced using general procedure D to afford **DP-61** as a brown solid, 65% yield; RP-HPLC (C18) 0−100% (ACN/water/0.1% TFA) in 8 min, t_R = 2.789 min, purity of 95%; ^{1}H NMR (500 MHz, DMSO-d_6) δ 8.70 (d, J = 5.2 Hz, 1H), 8.43 (s, 3H), 7.76−7.66 (m, 3H), 7.63 (dd, J = 5.3, 1.7 Hz, 1H), 7.54 (dd, J = 8.7, 2.3 Hz, 1H), 4.77 (ddt, J = 9.4, 6.3, 3.5 Hz, 1H), 4.28 (q, J = 5.7 Hz, 2H), 4.16 (t, J = 9.1 Hz, 1H), 3.91 (dd, J = 8.9, 6.0 Hz, 1H), 3.65 (ddd, J = 61.3, 12.4, 3.6 Hz, 2H); LCMS(ESI) $C_{16}H_{16}FN_3O_3$, $[M + H]^+$, m/z calcd 318.12, found 318.1.

(*R*)-3-(4-(6-(Aminomethyl)pyridin-3-yl)-3-fluorophenyl)-5-(hydroxymethyl)oxazolidin-2-one (DP-48). Using general procedure C, 5-bromopicolinonitrile and **3d** were employed to afford (*R*)-5-(2-fluoro-4-(5-(hydroxymethyl)-2-oxo-oxazolidin-3-yl)phenyl)picolinonitrile, which was then reduced using general procedure D to afford **DP-48** as a white solid, 87% yield; RP-HPLC (C18) 0−30% (ACN/water/0.1% TFA) in 30 min, t_R = 12.201 min, purity of 99%; ^{1}H NMR (500 MHz, DMSO-d_6) δ 8.81 (s, 1H), 8.40 (s, 2H), 8.07 (ddt, J = 8.2, 2.3, 1.1 Hz, 1H), 7.75−7.66 (m, 2H), 7.61 (d, J = 8.2 Hz, 1H), 7.51 (dd, J = 8.6, 2.2 Hz, 1H), 4.77 (ddd, J = 9.4, 6.3, 3.2 Hz, 1H), 4.27 (q, J = 5.7 Hz, 2H), 4.18−4.11 (m, 1H), 3.93−3.88 (m, 1H), 3.71 (dd, J = 12.4, 3.3 Hz, 1H), 3.62−3.57 (m, 2H); LCMS(ESI) $C_{16}H_{16}FN_3O_3$, $[M + H]^+$, m/z calcd 318.12, found 318.4.

(*R*)-3-(4-(6-(Aminomethyl)-5-fluoropyridin-3-yl)-3-fluorophenyl)-5-(hydroxymethyl)oxazolidin-2-one (DP-62). Using general procedure C, 5-bromo-3-fluoropicolinonitrile and **3d** were employed to afford (*R*)-3-fluoro-5-(2-fluoro-4-(5-(hydroxymethyl)-2-oxo-oxazolidin-3-yl)phenyl)picolinonitrile, which was then reduced using general procedure D to afford **DP-62** as a white solid, 91% yield; RP-HPLC (C18) 2−30% (ACN/water/0.1% TFA) in 30 min, t_R = 9.996 min, purity of 95%; LCMS(ESI) $C_{16}H_{15}F_2N_3O_3$, $[M + H]^+$, m/z calcd 336.11, found 336.1.

(*R*)-5-(2-Fluoro-4-(5-(hydroxymethyl)-2-oxo-oxazolidin-3-yl)phenyl)-3-hydroxypicolinonitrile (DP-300). 5-Bromo-3-fluoropicolinonitrile (0.201 g, 1 mmol) was dissolved in DMF (5 mL), and then NaOtBu (1.5 mmol) was added. The reaction mixture was stirred for 2 h at room temperature to afford 5-bromo-3-(*tert*-butoxy)picolinonitrile as evident by LC-MS. Then the crude was used for Suzuki coupling with **3d** using general procedure C to afford (*R*)-3-(*tert*-butoxy)-5-(2-fluoro-4-(5-(hydroxymethyl)-2-oxo-oxazolidin-3-yl)phenyl)-picolinonitrile, which was then dissolved in 1:1 DCM/TFA solvent mixture (5 mL) and stirred at room temperature for 30 min. Then the solvent was evaporated and the residue purified by reversed phase column chromatography on preparative HPLC using a gradient of water/acetonitrile/0.1% TFA. Those fractions containing pure product were pooled and lyophilized to afford **DP-300** as a yellow solid, 95% yield; RP-HPLC (C18) 2−50% (ACN/water/0.1% TFA) in 30 min, t_R = 14.978 min, purity of 97%; ^{1}H NMR (399 MHz, DMSO-d_6) δ 11.93 (s, 1H), 8.37 (d, J = 1.7 Hz, 1H), 7.71−7.64 (m, 1H), 7.60 (s, 1H), 7.54−7.47 (m, 1H), 7.42−7.36 (m, 1H), 4.74 (ddt, J = 9.5, 6.6, 3.7 Hz, 1H), 4.13 (t, J = 9.0 Hz, 1H), 3.88 (dd, J = 9.0, 6.0 Hz, 1H), 3.63 (ddd, J = 49.7, 12.4, 3.6 Hz, 2H); ^{19}F NMR (376 MHz, DMSO) δ −115.77; LCMS(ESI) $C_{16}H_{12}FN_3O_4$, $[M + H]^+$, m/z calcd 330.08, found 329.9.

(*R*)-3-Amino-5-(2-fluoro-4-(5-(hydroxymethyl)-2-oxo-oxazolidin-3-yl)phenyl)picolinonitrile (DP-63). Using general procedure C, 3-amino-5-bromopicolinonitrile and **3d** were employed to afford **DP-63** as a white solid, 91% yield; RP-HPLC (C18) 2−30% (ACN/water/0.1% TFA) in 30 min, t_R = 20.970 min, purity of 95%; ^{1}H NMR (500 MHz, DMSO-d_6) δ 8.07 (d, J = 1.7 Hz, 1H), 7.69 (dd, J = 13.7, 2.2 Hz, 1H), 7.64 (t, J = 8.8 Hz, 1H), 7.51 (dd, J = 8.6, 2.3 Hz, 1H), 7.41 (t, J = 1.6 Hz, 1H), 5.26 (t, J = 5.6 Hz, 1H), 4.76 (ddt, J = 9.5, 6.3, 3.4 Hz, 1H), 4.15 (t, J = 9.0 Hz, 1H), 3.89 (dd, J = 8.9, 6.0 Hz, 1H), 3.64 (dddd, J = 61.0, 12.3, 5.6, 3.6 Hz, 2H); LCMS(ESI) $C_{16}H_{13}FN_4O_3$, $[M + H]^+$, m/z calcd 329.10, found 329.1.

(*R*)-3-(4-(5-Amino-6-(aminomethyl)pyridin-3-yl)-3-fluorophenyl)-5-(hydroxymethyl)oxazolidin-2-one (DP-262). (*R*)-3-Amino-5-(2-fluoro-4-(5-(hydroxymethyl)-2-oxo-oxazolidin-3-yl)phenyl)picolinonitrile, **DP-63**, was reduced using general procedure D to afford **DP-262** as a light brown solid, 34% yield; RP-HPLC (C18) 2−30% (ACN/water/0.1% TFA) in 30 min, t_R = 8.789 min, purity of 97%; ^{1}H NMR (500 MHz, DMSO-d_6) δ 8.23 (s, 3H), 8.02 (t, J = 1.8 Hz, 1H), 7.66 (dd, J = 13.5, 2.3 Hz, 1H), 7.57 (t, J = 8.7 Hz, 1H), 7.48 (dd, J

DOI: 10.1021/acsinfecdis.6b00003
ACS Infect. Dis. 2016, 2, 405−426

= 8.6, 2.3 Hz, 1H), 7.25 (t, J = 1.7 Hz, 1H), 4.76 (ddt, J = 9.5, 6.5, 3.6 Hz, 1H), 4.14 (t, J = 9.0 Hz, 1H), 4.03 (d, J = 5.0 Hz, 2H), 3.89 (dd, J = 8.9, 6.1 Hz, 1H), 3.71 (dd, J = 12.4, 3.3 Hz, 2H); LCMS(ESI) $C_{16}H_{17}FN_4O_3$, $[M + H]^+$, m/z calcd 333.13, found 333.1.

(*R*)-3-(4-(6-(Aminomethyl)-5-hydroxypyridin-3-yl)-3-fluorophenyl)-5-(hydroxymethyl)oxazolidin-2-one (DP-326). (*R*)-5-(2-Fluoro-4-(5-(hydroxymethyl)-2-oxo-oxazolidin-3-yl)phenyl)-3-hydroxypicolinonitrile, **DP-300**, was reduced using general procedure D to afford **DP-326** as a yellow solid, 50% yield; RP-HPLC (C18) 2−30% (ACN/water/0.1% TFA) in 30 min, t_R = 9.849 min, purity of 95%; ^{1}H NMR (399 MHz, acetone-d_6) δ 8.30 (s, 1H), 7.79 (s, 1H), 7.76−7.69 (m, 1H), 7.68−7.52 (m, 1H), 7.46 (d, J = 7.8 Hz, 1H), 5.06 (s, 1H), 4.92−4.75 (m, 3H), 4.24 (t, J = 8.9 Hz, 1H), 4.06 (dd, J = 8.7, 6.2 Hz, 1H), 3.85 (ddd, J = 45.9, 12.3, 3.4 Hz, 2H); ^{19}F NMR (376 MHz, acetone) δ −117.12); LCMS(ESI) $C_{16}H_{16}FN_3O_4$, $[M + H]^+$, m/z calcd 334.11.

(*R*)-3-(4-(6-Amino-5-hydroxypyridin-3-yl)-3-fluorophenyl)-5-(hydroxymethyl)oxazolidin-2-one (DP-306). Using general procedure B, 2-amino-5-bromopyridin-3-ol and **3d** were employed to afford **DP-306** as a yellow solid, 45% yield; RP-HPLC (C18) 2−30% (ACN/water/0.1% TFA) in 30 min, t_R = 11.429 min, purity of 97%; ^{1}H NMR (399 MHz, DMSO-d_6) δ 11.59 (s, 1H), 7.84 (s, 2H), 7.63 (td, J = 7.1, 2.3 Hz, 2H), 7.54 (t, J = 8.8 Hz, 1H), 7.44 (dd, J = 8.7, 2.3 Hz, 1H), 7.35 (d, J = 1.7 Hz, 1H), 4.73 (ddt, J = 9.5, 6.6, 3.5 Hz, 1H), 4.10 (t, J = 9.0 Hz, 1H), 3.85 (dd, J = 9.0, 6.1 Hz, 1H), 3.73−3.49 (m, 2H); ^{19}F NMR (376 MHz, DMSO) δ −116.36; LCMS(ESI) $C_{15}H_{14}FN_3O_4$, $[M + H]^+$, m/z calcd 320.10, found 319.9.

(*R*)-3-Amino-5-(2-fluoro-4-(5-(hydroxymethyl)-2-oxo-oxazolidin-3-yl)phenyl)picolinic acid (DP-16). Using general procedure B, 3-amino-5-bromopicolinic acid and **3d** were employed to afford **DP-16** as a brown solid, 73% yield; RP-HPLC (C18) 0−100% (ACN/water/0.1% TFA) in 8 min, t_R = 2.775 min, purity of 70%; LCMS(ESI) $C_{16}H_{14}FN_3O_5$, $[M + H]^+$, m/z calcd 348.09, found; 348.1.

(*R*)-2-Amino-5-(2-fluoro-4-(5-(hydroxymethyl)-2-oxo-oxazolidin-3-yl)phenyl)nicotinic acid (DP-27). Using general procedure B, 2-amino-5-bromonicotinic acid and **3d** were employed to afford **DP-27** as a white solid, 68% yield; RP-HPLC (C18) 0−100% (ACN/water/0.1% TFA) in 8 min, t_R = 2.784 min, purity of 95%; ^{1}H NMR (500 MHz, DMSO-d_6) δ 8.40 (dd, J = 2.6, 1.5 Hz, 1H), 8.21 (dd, J = 2.6, 1.3 Hz, 1H), 7.68−7.55 (m, 2H), 7.43 (dd, J = 8.6, 2.3 Hz, 1H), 4.75 (td, J = 5.9, 2.8 Hz, 1H), 4.13 (t, J = 9.1 Hz, 1H), 3.88 (dd, J = 8.9, 6.1 Hz, 1H), 3.75−3.53 (m, 2H); LCMS(ESI) $C_{16}H_{14}FN_3O_5$, $[M + H]^+$, m/z calcd 348.09, found 348.1.

(*R*)-2,2′-Difluoro-5-hydroxy-4′-(5-(hydroxymethyl)-2-oxo-oxazolidin-3-yl)-[1,1′-biphenyl]-4-carbonitrile (DP-303). 4-Bromo-2,5-difluorobenzonitrile (1 mmol) was dissolved DMF (5 mL), and then NaOtBu (1.5 mmol) was added. The reaction mixture was stirred for 2 h at room temperature to afford 4-bromo-2-(*tert*-butoxy)-5-fluorobenzonitrile as evident by LC-MS. Then the crude was used for Suzuki coupling with **3d** using general procedure C to afford (*R*)-5-(*tert*-butoxy)-2,2′-difluoro-4′-(5-(hydroxymethyl)-2-oxo-oxazolidin-3-yl)-[1,1′-biphenyl]-4-carbonitrile, which was then dissolved in 1:1 DCM/TFA solvent mixture (5 mL) and stirred at room temperature for 30 min. Then the solvent was evaporated and the residue purified by reversed phase column chromatography on preparative HPLC using a gradient of water/acetonitrile/0.1% TFA. Those fractions containing pure product were pooled and lyophilized to afford **DP-303** as a white solid, 76% yield; RP-HPLC (C18) 2−100% (ACN/water/0.1% TFA) in 30 min, t_R = 11.159 min, purity of 97%; ^{1}H NMR (399 MHz, DMSO-d_6) δ 11.26 (d, J = 1.4 Hz, 1H), 7.72 (dd, J = 9.5, 1.7 Hz, 1H), 7.66−7.60 (m, 1H), 7.53−7.44 (m, 2H), 6.99 (d, J = 6.1 Hz, 1H), 5.23 (s, 1H), 4.72 (m, J = 7.8 Hz, 1H), 4.20−4.07 (m, 1H), 3.86 (dd, J = 8.7, 5.9 Hz, 1H), 3.67 (d, J = 12.5 Hz, 1H), 3.55 (d, J = 12.0 Hz, 1H); LCMS(ESI) $C_{17}H_{12}F_2N_2O_4$, $[M + H]^+$, m/z calcd 347.08, found 346.9.

(*R*)-5-(Hydroxymethyl)-3-(2,2′,4′-trifluoro-3′-hydroxy-[1,1′-biphenyl]-4-yl)oxazolidin-2-one (DP-316). Using general procedure B, 3-bromo-2,6-difluorophenol and **3d** were employed to afford **DP-316** as a yellow oil, 30% yield; RP-HPLC (C18) 2−98% (ACN/water/0.1% TFA) in 30 min, t_R = 17.584 min, purity of 99%; ^{1}H NMR (399 MHz, acetone-d_6) δ 10.31 (s, 1H), 7.61−7.58 (d, J = 12 Hz, 1H), 7.45−7.39 (m, J = 9.2, 8.8, 6.8 Hz, 2H), 7.13−7.08 (td, J = 9.8, 1.2 Hz, 1H), 6.84−6.79 (dd, J = 14, 8 Hz, Hz, 1 H), 5.21 (s, 1H), 4.72−4.71 (m, J = 3.6 Hz, 1H), 4.10 (t, J = 8.8 Hz, 1H), 3.87−3.83 (dd, J = 8.8, 6.4 Hz, 1H), 3.68 (d, J = 12 Hz, 1H), 3.56 (d, J = 12 Hz, 1H); LCMS(ESI) $C_{16}H_{12}F_3NO_4$, $[M + H]^+$, m/z calcd 340.07, found 339.9.

(*R*)-3-(4′-(Aminomethyl)-2,2′-difluoro-5′-hydroxy-[1,1′-biphenyl]-4-yl)-5-(hydroxymethyl)oxazolidin-2-one (DP-325). (*R*)-2,2′-Fifluoro-5-hydroxy-4′-(5-(hydroxymethyl)-2-oxo-oxazolidin-3-yl)-[1,1′-biphenyl]-4-carbonitrile, **DP-303**, was reduced using general procedure D to afford **DP-325** as a dark brown solid, 100% yield; RP-HPLC (C18) 2−30% (ACN/water/0.1% TFA) in 30 min, t_R = 14.6727 min, purity of 92%; ^{1}H NMR (500 MHz, DMSO-d_6) δ 10.38 (s, 1H), 8.13 (s, 2H), 7.65 (d, J = 2.2 Hz, 1H), 7.60−7.41 (m, 2H), 7.31 (d, J = 10.2 Hz, 1H), 6.91 (d, J = 6.4 Hz, 1H), 5.27 (t, J = 5.8 Hz, 1H), 4.76 (m, J = 6.0, 2.9 Hz, 1H), 4.14 (t, J = 9.2 Hz, 2H), 4.02 (s, 2H), 3.89 (dd, J = 9.0, 5.9 Hz, 1H); LCMS(ESI) $C_{17}H_{16}F_2N_2O_4$, $[M + H]^+$, m/z calcd 351.07, found 350.9.

(*R*)-3-(3′-(Aminomethyl)-2-fluoro-4′-hydroxy-[1,1′-biphenyl]-4-yl)-5-(hydroxymethyl)oxazolidin-2-one (DP-17). (*R*)-2′-Fluoro-4-hydroxy-4′-(5-(hydroxymethyl)-2-oxo-oxazolidin-3-yl)-[1,1′-biphenyl]-3-carbonitrile, **DP-2**, was reduced using general procedure D to afford **DP-17** as a tan solid, 53% yield; RP-HPLC (C18) 2−30% (ACN/water/0.1% TFA) in 30 min, t_R = 14.967 min, purity of 98%; ^{1}H NMR (399 MHz, acetone-d_6) δ 7.68 (dd, J = 13.8, 2.3 Hz, 1H), 7.60 (s, 1H), 7.51 (t, J = 8.8 Hz, 1H), 7.42 (dd, J = 21.0, 8.2 Hz, 2H), 7.10 (d, J = 8.5 Hz, 1H), 5.01 (s, 2H), 4.86−4.76 (m, 1H), 4.22 (t, J = 8.9 Hz, 1H), 4.03 (dd, J = 8.8, 6.2 Hz, 1H), 3.93−3.73 (m, 2H); ^{19}F NMR (376 MHz, acetone) δ −118.01; LCMS(ESI) $C_{17}H_{17}FN_2O_4$, $[M + H]^+$, m/z calcd 333.12, found 333.1.

(*R*)-3-(4′-(Aminomethyl)-2-fluoro-3′-hydroxy-[1,1′-biphenyl]-4-yl)-5-(hydroxymethyl)oxazolidin-2-one (DP-19). (*R*)-2′-Fluoro-3-hydroxy-4′-(5-(hydroxymethyl)-2-oxo-oxazolidin-3-yl)-[1,1′-biphenyl]-4-carbonitrile, **DP-3**, was reduced using general procedure D to afford **DP-19** as a tan solid, 40% yield; RP-HPLC (C18) 0−30% (ACN/water/0.1% TFA) in 30 min, t_R = 14.937 min, purity of 96%; ^{1}H NMR (399 MHz, acetone-d_6) δ 7.67 (dd, J = 13.7, 2.2 Hz, 1H), 7.50−7.34 (m, 3H), 7.25 (d, J = 3.4 Hz, 1H), 7.06−6.99 (m, 1H), 4.97 (s, 2H), 4.81 (ddt, J = 9.6, 6.9, 3.7 Hz, 1H), 4.20 (t, J = 8.9 Hz, 1H), 4.03 (dd, J = 8.8, 6.2 Hz, 1H), 3.82 (ddd, J = 47.8, 12.3, 3.6 Hz, 2H); ^{13}C NMR (100 MHz, acetone) δ 161.00, 158.55, 156.21, 156.14, 154.67, 140.38, 137.59, 131.00, 130.89, 130.84,

DOI: 10.1021/acsinfecdis.6b00003
ACS Infect. Dis. 2016, 2, 405−426

122.69, 120.26, 119.01, 116.52, 113.66, 105.73, 105.44, 73.67, 62.35, 46.67, 46.31; ^{19}F NMR (376 MHz, acetone) δ −117.30; ; LCMS(ESI) $C_{17}H_{17}FN_2O_4$, $[M - H]^-$, m/z calcd 331.12, found 331.1.

(*R*)-3-(3′-(Aminomethyl)-2-fluoro-5′-hydroxy-[1,1′-biphenyl]-4-yl)-5-(hydroxymethyl)oxazolidin-2-one (DP-366). (*R*)-2′-Fluoro-5-hydroxy-4′-(5-(hydroxymethyl)-2-oxo-oxazolidin-3-yl)-[1,1′-biphenyl]-3-carbonitrile, **DP-365**, was reduced using general procedure D to afford **DP-366** as a pale yellow solid, 75% yield; RP-HPLC (C18) 2−30% (ACN/water/0.1% TFA) in 30 min, t_R = 12.643 min, purity of 100%; ^{1}H NMR (399 MHz, methanol-d_4) δ 7.63 (dd, J = 13.3, 2.3 Hz, 1H), 7.50 (t, J = 8.6 Hz, 1H), 7.40 (dd, J = 8.6, 2.3 Hz, 1H), 7.12−7.07 (m, 1H), 7.03 (q, J = 1.8 Hz, 1H), 6.88 (t, J = 2.0 Hz, 1H), 4.78 (ddt, J = 9.7, 6.8, 3.6 Hz, 1H), 4.16 (t, J = 9.0 Hz, 1H), 4.09 (s, 2H), 3.97 (td, J = 6.3, 3.1 Hz, 1H), 3.79 (ddd, J = 66.9, 12.5, 3.5 Hz, 2H); ^{19}F NMR (376 MHz, CD_3OD) δ −117.72; LCMS(ESI) $C_{17}H_{17}FN_2O_4$, $[M + H]^+$, m/z calcd 333.12, found 332.8.

(*R*)-3-(2-Fluoro-3′-hydroxy-4′-(hydroxymethyl)-[1,1′-biphenyl]-4-yl)-5-(hydroxymethyl)oxazolidin-2-one (DP-324). (*R*)-2′-Fluoro-3-hydroxy-4′-(5-(hydroxymethyl)-2-oxo-oxazolidin-3-yl)-[1,1′-biphenyl]-4-carbaldehyde, **DP-319** (1 mmol), was dissolved in anhydrous MeOH (2 mL), then sodium cyanoborohydride (1.5 equiv) was added in portions, and the reaction was stirred at room temperature for 12 h. DDW (5 mL) was then added, and the mixture was extracted in EtOAc (3 × 5 mL). The organic layers were combined, dried over Na_2SO_4, and concentrated under vacuum. The residue was then purified by reversed phase column chromatography on preparative HPLC using a gradient of water/acetonitrile/0.1% TFA. Those fractions containing pure product were pooled and lyophilized to afford **DP-324** as a tan solid, 75% yield; RP-HPLC (C18) 2−50% (ACN/water/0.1% TFA) in 30 min, t_R = 13.012 min, purity of 100%; ^{1}H NMR (399 MHz, acetone-d_6) δ 7.67 (dd, J = 13.7, 2.2 Hz, 1H), 7.50 (t, J = 8.7 Hz, 1H), 7.42 (dd, J = 8.6, 2.3 Hz, 1H), 7.34 (d, J = 7.7 Hz, 1H), 7.06−6.99 (m, 2H), 4.85−4.80 (m, 1H), 4.79 (s, 2H), 4.22 (t, J = 8.9 Hz, 1H), 4.03 (dd, J = 8.8, 6.2 Hz, 1H), 3.84 (ddd, J = 50.4, 12.3, 3.7 Hz, 2H); ^{13}C NMR (100 MHz, acetone) δ 161.02, 155.39, 154.65, 139.97, 135.32, 130.88, 127.89, 127.24, 123.32, 120.00, 115.73, 113.64, 105.75, 105.46, 73.65, 62.51, 60.82, 46.32; ^{19}F NMR (376 MHz, acetone) δ −117.47; LCMS(ESI) $C_{17}H_{16}FNO_5$, $[M + H]^+$, m/z calcd 334.10, found 333.9.

(*R*)-2′-Fluoro-3-hydroxy-4′-(5-(hydroxymethyl)-2-oxo-oxazolidin-3-yl)-[1,1′-biphenyl]-4-carboxamide (DP-264). Methyl 4-bromo-2-hydroxybenzoate (1 mmol) was dissolved in NH_4OH (10 mL) and heated in a pressure flask at 100 °C for 48 h. Then solvent was evaporated to dryness to afford 4-bromo-2-hydroxybenzamide as a creamy solid as evident by LC-MS. Then the residue was used for Suzuki coupling with **3d** using general procedure B to afford **DP-264** as a creamy solid, 86% yield; RP-HPLC (C18) 2−100% (ACN/water/0.1% TFA) in 30 min, t_R = 8.789 min, purity of 99%; ^{1}H NMR (399 MHz, DMSO-d_6) δ 8.43 (s, 1H), 7.94 (s, 1H), 7.91 (d, J = 8.5 Hz, 1H), 7.64−7.57 (m, 2H), 7.44 (dd, J = 8.6, 2.2 Hz, 1H), 7.04 (d, J = 5.6 Hz, 2H), 4.77−4.63 (m, 1H), 4.11 (t, J = 9.0 Hz, 1H), 3.86 (dd, J = 8.9, 6.1 Hz, 1H), 3.62 (ddd, J = 49.2, 12.4, 3.6 Hz, 2H); ^{19}F NMR (376 MHz, acetone) δ −116.33; LCMS(ESI) $C_{17}H_{15}FN_2O_5$, $[M + H]^+$, m/z calcd 347.10, found 347.1.

(*R*)-2′-Fluoro-4-hydroxy-4′-(5-(hydroxymethyl)-2-oxo-oxazolidin-3-yl)-[1,1′-biphenyl]-3-carboxamide (DP-278). Methyl 5-bromo-2-hydroxybenzoate (1 mmol) was dissolved in NH_4OH (10 mL) and heated in a pressure flask at 100 °C for 48 h. Then solvent was evaporated to dryness to afford 5-bromo-2-hydroxybenzamide as a white solid as evident by LC-MS. Then the residue was used for Suzuki coupling with **3d** using general procedure B to afford **DP-278** as a white solid, 30% yield; RP-HPLC (C18) 2−50% (ACN/water/0.1% TFA) in 30 min, t_R = 15.984 min, purity of 98%; ^{1}H NMR (399 MHz, methanol-d_4) δ 7.98 (m, 1H), 7.63 (d, J = 2.2 Hz, 1H), 7.61−7.56 (m, 1H), 7.41 (d, J = 1.8 Hz, 2H), 6.98 (d, J = 8.6 Hz, 1H), 4.80−4.73 (m, 1H), 4.17 (td, J = 9.0, 3.7 Hz, 1H), 3.97 (ddd, J = 9.2, 6.4, 3.1 Hz, 1H), 3.92−3.66 (m, 2H); ^{19}F NMR (376 MHz, CD_3OD) δ −118.28; LCMS(ESI) $C_{17}H_{15}FN_2O_5$, $[M + H]^+$, m/z calcd 347.1, found 347.1.

(*R*)-2′-Fluoro-3-hydroxy-4′-(5-(hydroxymethyl)-2-oxo-oxazolidin-3-yl)-[1,1′-biphenyl]-4-carboxylic acid (DP-279). Using general procedure B, 4-bromo-2-hydroxybenzoic acid and **3d** were employed to afford **DP-279** as a light brown solid, 35% yield; RP-HPLC (C18) 2−50% (ACN/water/0.1% TFA) in 30 min, t_R = 16.844 min, purity of 99%; ^{1}H NMR (399 MHz, acetone-d_6) δ 7.97 (d, J = 8.1 Hz, 1H), 7.73 (dd, J = 13.9, 2.2 Hz, 1H), 7.62 (t, J = 8.7 Hz, 1H), 7.50 (dd, J = 8.6, 2.3 Hz, 1H), 7.17 (d, J = 8.5 Hz, 2H), 4.84 (ddt, J = 9.7, 6.9, 3.7 Hz, 1H), 4.25 (t, J = 8.9 Hz, 1H), 4.06 (dd, J = 8.8, 6.2 Hz, 1H), 3.85 (ddd, J = 51.0, 12.3, 3.7 Hz, 2H); ^{19}F NMR (376 MHz, acetone) δ −116.77; LCMS(ESI) $C_{17}H_{14}FNO_6$, $[M + H]^+$, m/z calcd 348.08, found 348.4.

(*R*)-2′-Fluoro-4-hydroxy-4′-(5-(hydroxymethyl)-2-oxo-oxazolidin-3-yl)-[1,1′-biphenyl]-3-carboxylic acid (DP-280). Using general procedure B, 5-bromo-2-hydroxybenzoic acid and **3d** were employed to afford **DP-280** as a white solid, 85% yield; RP-HPLC (C18) 2−50% (ACN/water/0.1% TFA) in 30 min, t_R = 17.660 min, purity of 99%; ^{1}H NMR (399 MHz, acetone-d_6) δ 11.18 (s, 1H), 8.14−8.04 (m, 1H), 7.79−7.66 (m, 1H), 7.55 (t, J = 8.8 Hz, 1H), 7.45 (dd, J = 8.6, 2.3 Hz, 1H), 7.07 (d, J = 8.7 Hz, 1H), 4.82 (ddt, J = 9.6, 6.7, 3.6 Hz, 1H), 4.23 (t, J = 8.9 Hz, 1H), 4.05 (dd, J = 8.8, 6.2 Hz, 1H), 3.85 (ddd, J = 51.2, 12.4, 3.7 Hz, 2H); ^{13}C NMR (100 MHz, acetone) δ 171.87, 161.80, 160.97, 158.54, 154.63, 140.18, 136.45, 130.67, 130.61, 126.57, 117.80, 113.79, 112.59, 105.75, 105.46, 73.65, 62.50, 46.30; ^{19}F NMR (376 MHz, acetone) δ −118.22; LCMS(ESI) $C_{17}H_{14}FNO_6$, $[M + H]^+$, m/z calcd 348.08, found 348.0.

(*R*)-3-(2-Fluoro-3′,5′-dihydroxy-[1,1′-biphenyl]-4-yl)-5-(hydroxymethyl)oxazolidin-2-one (DP-304). Using general procedure C, 5-bromoresorcinol and **3d** were employed to afford **DP-304** as a white solid, 40% yield; RP-HPLC (C18) 2−50% (ACN/water/0.1% TFA) in 30 min, t_R = 12.545 min, purity of 95%; LCMS(ESI) $C_{16}H_{14}FNO_5$, $[M + H]^+$, m/z calcd 320.09, found 319.9.

((*R*)-*N*-(2′-Fluoro-4-hydroxy-4′-(5-(hydroxymethyl)-2-oxo-oxazolidin-3-yl)-[1,1′-biphenyl]-3-yl)acetamide (DP-307). 2-Amino-4-bromophenol (1 mmol) and imidazole (2 mmol) were dissolved in anhydrous DCM (2 mL) and then cooled to 0 °C in an ice bath. Then *tert*-butylchlorodimethylsilane (1.2 mmol) was dissolved in anhydrous DCM (1 mL) and then added dropwise to the reaction mixture at 0 °C. The reaction was allowed to warm gradually to room temperature under stirring for 2 h. Then it was extracted with DDW (3 × 5 mL). The orgnic layer was then dried over sodium sulfate and concentrated under vacuum to afford 4-bromo-2-((*tert*-butyldimethylsilyl)oxy)aniline as a brown solid as evident by LC-MS. The product was then dissolved in acetic anhydride (2

DOI: 10.1021/acsinfecdis.6b00003
ACS Infect. Dis. 2016, 2, 405−426

mL) and stirred at room temperature overnight. Then solvent was evaporated to dryness to get *N*-(5-bromo-2-((*tert*-butyldimethylsilyl)oxy)phenyl)acetamide as a yellow oil as evident by LC-MS. Then this product was used for Suzuki coupling with **3d** using general procedure C, and the reaction time was extended to 12 h to afford **DP-307** as a white solid, 90% yield; RP-HPLC (C18) 2−50% (ACN/water/0.1% TFA) in 30 min, t_R = 13.542 min, purity of 99%; ^{1}H NMR (399 MHz, methanol-d_4) δ 7.85 (s, 1H), 7.59 (d, J = 13.0 Hz, 1H), 7.46 (t, J = 8.7 Hz, 1H), 7.35 (d, J = 8.7 Hz, 1H), 7.21 (d, J = 8.6 Hz, 1H), 6.93 (d, J = 8.4 Hz, 1H), 4.86 (m, 1H), 4.16 (t, J = 9.1 Hz, 1H), 4.01−3.92 (m, 1H), 3.94−3.63 (m, 2H); ^{19}F NMR (376 MHz, CD_3OD) δ −118.20; LCMS(ESI) $C_{18}H_{17}FN_2O_5$, $[M + H]^+$, m/z calcd 361.11, found 360.9.

(*R*)-2′-Fluoro-*N*′,3-dihydroxy-4′-(5-(hydroxymethyl)-2-oxo-oxazolidin-3-yl)-[1,1′-biphenyl]-4-carboximidamide (DP-321). (*R*)-2′-Fluoro-3-hydroxy-4′-(5-(hydroxymethyl)-2-oxo-oxazolidin-3-yl)-[1,1′-biphenyl]-4-carbonitrile, **DP-3** (1 mmol), was added to a nitrogen-purged round-bottom flask along with 50% hydroxylamine hydrochloride in water (1 mmol) and sodium hydroxide (0.400 g, 1 mmol). The solids were then dissolved in ethanol (2 mL), and the reaction mixture was heated to 80 °C and stirred for 2 h. Then solvent was removed under vacuum, and the resulting residue was dissolved in EtOAc (5 mL) and then extracted with DDW (3 × 5 mL); the organic layer was dried using Na_2SO_4 and concentrated under vacuum to afford **DP-321** as a light brown solid, 97% yield; RP-HPLC (C18) 2−50% (ACN/water/0.1% TFA) in 30 min, t_R = 9.631 min, purity of 100%; ^{1}H NMR (399 MHz, DMSO-d_6) δ 10.70 (s, 1H), 10.10 (s, 1H), 7.63 (d, J = 2.2 Hz, 1H), 7.61−7.51 (m, 2H), 7.44 (dd, J = 8.7, 2.2 Hz, 1H), 7.13−7.03 (m, 3H), 5.21 (s, 1H), 4.72 (td, J = 5.9, 2.8 Hz, 1H), 4.10 (t, J = 9.1 Hz, 1H), 3.85 (dd, J = 8.9, 6.0 Hz, 1H), 3.67 (dd, J = 12.4, 3.3 Hz, 1H), 3.54 (dd, J = 12.4, 3.9 Hz, 1H); LCMS(ESI) $C_{17}H_{16}FN_3O_5$, $[M + H]^+$, m/z calcd 362.11, found 362.9.

((2′-Fluoro-3-hydroxy-4′-((*R*)-5-(hydroxymethyl)-2-oxo-oxazolidin-3-yl)-[1,1′-biphenyl]-4-yl)methyl)alanine (DP-323). (*R*)-2′-Fluoro-3-hydroxy-4′-(5-(hydroxymethyl)-2-oxo-oxazolidin-3-yl)-[1,1′-biphenyl]-4-carbaldehyde, **DP-319** (1 mmol), was dissolved in anhydrous MeOH (2 mL), and then AcOH (2 mL) and L-alanine (1 mmol) were added, and the reaction was stirred at room temperature for 15 min. The reaction mixture was then cooled to 0 °C in an ice bath, and then sodium cyanoborohydride was cautionly added, and the cooling bath was removed. The reaction mixture was stirred at room temperature for 30 min. Acetone (5 mL) was added, and the produced emulsion was centrifuged to get **DP-323** as a yellow precipitate, which was filtered, washed with DDW (3 × 5 mL), and dried under vacuum, 60% yield; RP-HPLC (C18) 2−30% (ACN/water/0.1% TFA) in 30 min, t_R = 15.422 min, purity of 100%; ^{1}H NMR (399 MHz, methanol-d_4) δ 7.17 (t, J = 8.7 Hz, 1H), 7.04 (d, J = 7.8 Hz, 1H), 6.85 (t, J = 1.6 Hz, 1H), 6.80 (d, J = 7.7 Hz, 1H), 6.50 (dd, J = 8.5, 2.3 Hz, 1H), 6.42 (dd, J = 13.7, 2.3 Hz, 1H), 3.98 (d, J = 13.4 Hz, 1H), 3.83 (p, J = 5.5 Hz, 1H), 3.75 (d, J = 13.5 Hz, 1H), 3.59 (dd, J = 7.4, 5.3 Hz, 1H), 3.21 (q, J = 7.0 Hz, 1H), 3.09 (dd, J = 13.2, 6.9 Hz, 1H), 1.31 (d, J = 7.0 Hz, 3H); ^{19}F NMR (376 MHz, CD_3OD) δ −119.37; LCMS(ESI) $C_{20}H_{21}FN_2O_6$, $[M + H]^+$, m/z calcd 405.14, found 404.9.

(*R*)-2-(Dimethylamino)-*N*-(2′-fluoro-3-hydroxy-4′-(5-(hydroxymethyl)-2-oxo-oxazolidin-3-yl)-[1,1′-biphenyl]-4-yl)acetamide (DP-330). A mixture of BiBop (1.3 mmol), DIPEA (2 mmol), and (dimethylamine)acetic acid (1 mmol) in anhydrous DMF (2 mL) was stirred at room temperature for 30 min. Then 4-bromo-2-((*tert*-butyldimethylsilyl)oxy)aniline (1 mmol) was added, and the reaction mixture was stirred at room temperature for 1 h to produce *N*-(4-bromo-2-((*tert*-butyldimethylsilyl)oxy)phenyl)-2-(dimethylamino)acetamide as evident by LC-MS. Then the crude was used for Suzuki coupling with **3d** using general procedure C with the reaction time extended to 12 h to afford **DP-330** as a white solid, 95% yield; RP-HPLC (C18) 2−30% (ACN/water/0.1% TFA) in 30 min, t_R = 13.370 min, purity of 98%; ^{1}H NMR (399 MHz, D_2O) δ 7.44 (d, J = 8.3 Hz, 1H), 6.99−6.86 (m, 2H), 6.79 (s, 1H), 6.74 (dd, J = 8.7, 2.5 Hz, 1H), 6.61 (d, J = 8.4 Hz, 1H), 4.45 (d, J = 7.4 Hz, 1H), 4.05 (s, 2H), 3.72−3.52 (m, 2H), 3.46−3.29 (m, 2H), 2.86 (s, 6H); ^{19}F NMR (376 MHz, D_2O) δ −116.25; LCMS(ESI) $C_{20}H_{22}FN_3O_5$, $[M + H]^+$, m/z calcd 404.15, found 403.7.

(*R*)-3-(4′-(((2-(Dimethylamino)ethyl)amino)methyl)-2-fluoro-3′-hydroxy-[1,1′-biphenyl]-4-yl)-5-(hydroxymethyl)oxazolidin-2-one (DP-335). (*R*)-2′-Fluoro-3-hydroxy-4′-(5-(hydroxymethyl)-2-oxo-oxazolidin-3-yl)-[1,1′-biphenyl]-4-carbaldehyde, **DP-319** (1 mmol), was dissolved in anhydrous MeOH (2 mL), and then AcOH (2 mL) and *N*,*N*-dimethylethylenediamine (1 mmol) were added, and the reaction was stirred at room temperature for 15 min. The reaction mixture was then cooled to 0 °C in an ice bath, and then sodium cyanoborohydride was cautionly added, and the cooling bath was removed. The reaction mixture was stirred at room temperature for 12 h. The residue was then purified by reversed phase column chromatography on preparative HPLC using a gradient of water/acetonitrile/0.1% TFA. Those fractions containing pure product were pooled and lyophilized to afford **DP-335** as a white solid, 95% yield; RP-HPLC (C18) 2−30% (ACN/water/0.1% TFA) in 30 min, t_R = 13.151 min, purity of 99%; ^{1}H NMR (399 MHz, deuterium oxide) δ 7.22 (d, J = 7.9 Hz, 1H), 7.18 (t, J = 8.8 Hz, 1H), 7.10 (dd, J = 13.3, 2.3 Hz, 1H), 6.97 (dd, J = 8.6, 2.3 Hz, 1H), 6.93 (t, J = 1.4 Hz, 1H), 6.90 (dd, J = 7.8, 1.6 Hz, 1H), 4.55 (dtt, J = 6.8, 5.2, 2.8 Hz, 1H), 4.18 (s, 2H), 3.83 (t, J = 9.2 Hz, 1H), 3.68 (dd, J = 12.9, 2.8 Hz, 1H), 3.57 (dd, J = 9.2, 6.5 Hz, 1H), 3.52−3.44 (m, 1H), 3.46−3.36 (m, 2H), 2.82 (s, 6H); ^{19}F NMR (376 MHz, D_2O) δ −116.49; LCMS(ESI) $C_{21}H_{26}FN_3O_4$, $[M + H]^+$, m/z calcd 404.19, found 404.0.

(*R*)-3-(4′-(((2-Aminoethyl)amino)methyl)-2-fluoro-3′-hydroxy-[1,1′-biphenyl]-4-yl)-5-(hydroxymethyl)-oxazolidin-2-one (DP-336). (*R*)-2′-Fluoro-3-hydroxy-4′-(5-(hydroxymethyl)-2-oxo-oxazolidin-3-yl)-[1,1′-biphenyl]-4-carbaldehyde, **DP-319** (1 mmol), was dissolved in anhydrous MeOH (2 mL), then AcOH (2 mL) and *N*,*N*-dimethylethylene diamine (1 mmol) were added, and the reaction was stirred at room temperature for 15 min. The reaction mixture was then cooled to 0 °C in an ice bath, then sodium cyanoborohydride was cautionly added, and the cooling bath was removed. The reaction mixture was stirred at room temperature for 12 h. Then solvent was evaporated to dryness, and the residue was then dissolved in a 1:1 DCM/TFA solvent mixture (5 mL) and stirred at room temperature for 30 min. Then the solvent was evaporated, and the residue was then purified by reversed phase column chromatography on preparative HPLC using a gradient of water/acetonitrile/0.1% TFA. Those fractions containing pure product were pooled and lyophilized to afford **DP-336** as a white solid, 80% yield; RP-HPLC (C18) 2−50% (ACN/water/0.1% TFA) in 30 min, t_R = 10.055 min, purity of 99%;

DOI: 10.1021/acsinfecdis.6b00003
ACS Infect. Dis. 2016, 2, 405−426

^{1}H NMR (399 MHz, deuterium oxide) δ 7.44−7.32 (m, 1H), 7.29 (dd, J = 8.3, 2.1 Hz, 1H), 7.21 (dd, J = 8.6, 2.4 Hz, 1H), 7.09−6.98 (m, 1H), 4.20 (s, 2H), 4.08 (t, J = 9.2 Hz, 1H), 3.86−3.72 (m, 2H), 3.61 (dd, J = 12.8, 4.3 Hz, 1H), 3.39−3.22 (m, 4H), 2.51 (p, J = 2.0 Hz, 1H); ^{19}F NMR (376 MHz, D_2O) δ −116.86; LCMS(ESI) $C_{19}H_{22}FN_3O_4$, $[M + H]^+$, m/z calcd 376.16, found 376.0.

(*R*)-3-(4′-((Dimethylamino)methyl)-2-fluoro-3′-hydroxy-[1,1′-biphenyl]-4-yl)-5-(hydroxymethyl)-oxazolidin-2-one (DP-470). ((*R*)-3-(4′-(Aminomethyl)-2-fluoro-3′-hydroxy-[1,1′-biphenyl]-4-yl)-5-(hydroxymethyl)-oxazolidin-2-one, **DP-19** (1 mmol), was dissolved in methanol (1 mL), then formaldehyde (0.70 mmol) was added, and the reaction mixture was stirred at room temperature for 30 min. Sodium cyanoborohydride (2 mmol) was then added slowly, and the reaction was stirred at room temperature for 2 h. Then DDW (5 mL) was added, and the mixture was then extracted with EtOAc (3 × 5 mL). Then organic layers were combined, dried over sodium sulfate, and concentrated under vacuum. The resulting crude mixture was dissolved in DMF (1 mL) and purified on a reverse-phase preparative HPLC system (water/acetonitrile/0.1% TFA), and the pure fractions were combined and lyophilized to afford **DP-470** as a white solid, 99% yield; RP-HPLC (C18) 2−50% (ACN/water/0.1% TFA) in 30 min, t_R = 10.805 min, purity of 100%; ^{1}H NMR LCMS(ESI) $C_{19}H_{21}FN_2O_4$, $[M + H]^+$, m/z calcd 361.15, found 361.8.

AUTHOR INFORMATION

Corresponding Author

*(J.B.A.) E-mail: james.b.aggen@gmail.com.

Present Addresses

$^{\Delta}$(H.D.C.) Rexahn Pharmaceuticals, Inc., Rockville, MD 20850, USA.

$^{\Pi}$(D.C.C.) Spring Bank Pharmaceuticals, Milford, MA 01757, USA.

$^{\Sigma}$(J.B.A.) Revolution Medicines, Redwood City, CA 94064, USA.

Funding

Funding for J.B.A, Defense Threat Reduction Agency Award HDTRA1-14-1-0019. Funding for P.J.B., American Cancer Society (Research Scholar Grant RSG-12-161-01-DMC). Funding for B.K., NU Office of the Provost Dissertation Grant.

Notes

A portion of this study was presented at the 55th Interscience Conference on Antimicrobial Agents and Chemotherapy, San Diego, CA, USA, September 17−21, 2015.

The authors declare no competing financial interest.

ACKNOWLEDGMENTS

We thank Dr. Vincent H. Tam from the University of Houston for the gift of MG1655 and MG1655 Δ*acrAB* used in the experiments.

REFERENCES

(1) Peleg, A. Y., and Hooper, D. C. (2010) Hospital-acquired infections due to Gram-negative bacteria. *N. Engl. J. Med. 362*, 1804−1813.

(2) Spellberg, B., Guidos, R., Gilbert, D., Bradley, J., Boucher, H. W., Scheld, W. M., et al. (2008) The epidemic of antibiotic-resistant infections: a call to action for the medical community from the Infectious Diseases Society of America. *Clin. Infect. Dis. 46*, 155−164.

(3) Hampton, T. (2013) Report reveals scope of US antibiotic resistance threat. *JAMA 310*, 1661−1663.

(4) Boucher, H. W., Talbot, G. H., Benjamin, D. K., Jr., Bradley, J., Guidos, R. J., Jones, R. N., et al. (2013) 10 × '20 Progress—development of new drugs active against Gram-negative bacilli: an update from the Infectious Diseases Society of America. *Clin. Infect. Dis. 56*, 1685−1694.

(5) Spellberg, B., and Shlaes, D. (2014) Prioritized current unmet needs for antibacterial therapies. *Clin. Pharmacol. Ther. 96*, 151−153.

(6) Silver, L. L. (2011) Challenges of antibacterial discovery. *Clin. Microbiol. Rev. 24* (1), 71−109.

(7) Nikaido, H. (2003) Molecular basis of bacterial outer membrane permeability revisited. *Microbiol. Mol. Biol. Rev. 67* (4), 593−656.

(8) Nakae, T., Ishii, J. N., Tokunaga, H., Kobayashi, Y., and Nakae, R. (1982) The solute selectivity of porin pores of *Escherichia coli* and *Salmonella typhimurium*. *Tokai J. Exp. Clin. Med. 7* (Suppl.), 141−148.

(9) Nikaido, H., and Thanassi, D. G. (1993) Penetration of lipophilic agents with multiple protonation sites into bacterial cells: tetracyclines and fluoroquinolones as examples. *Antimicrob. Agents Chemother. 37*, 1393−1399.

(10) Manchester, J. I., Buurman, E. T., Bisacchi, G. S., and McLaughlin, R. E. (2012) Molecular determinants of AcrB-mediated bacterial efflux implications for drug discovery. *J. Med. Chem. 55*, 2532−2537.

(11) O'Shea, R., and Moser, H. E. (2008) Physicochemical properties of antibacterial compounds: implications for drug discovery. *J. Med. Chem. 51* (10), 2871−2878.

(12) Domagala, J. M., Hanna, L. D., Heifetz, C. L., Hutt, M. P., Mich, T. F., Sanchez, J. P., et al. (1986) New structure-activity relationships of the quinolone antibacterials using the target enzyme. The development and application of a DNA gyrase assay. *J. Med. Chem. 29*, 394−404.

(13) Brown, D. G., May-Dracka, T. L., Gagnon, M. M., and Tommasi, R. (2014) Trends and exceptions of physical properties on antibacterial activity for Gram-positive and Gram-negative pathogens. *J. Med. Chem. 57*, 10144−10161.

(14) Tommasi, R., Brown, D. G., Walkup, G. K., Manchester, J. I., and Miller, A. A. (2015) ESKAPEing the labyrinth of antibacterial discovery. *Nat. Rev. Drug Discovery 14*, 529.

(15) Michalska, K., Karpiuk, I., Krol, M., and Tyski, S. (2013) Recent development of potent analogues of oxazolidinone antibacterial agents. *Bioorg. Med. Chem. 21*, 577−591.

(16) Guo, B., Fan, H., Xin, Q., Chu, W., Wang, H., Huang, Y., Chen, X., and Yang, Y. (2013) Solubility-Driven Optimization of (Pyridin-3-yl) Benzoxazinyloxazolidinones Leading to a Promising Antibacterial Agent. *J. Med. Chem. 56*, 2642−2650.

(17) Srivastava, B. K., Soni, R., Patel, J. Z., Jain, M. R., and Patel, P. R. (2008) Oxazolidinone Antibacterials and Our Experience. *Anti-Infect. Agents Med. Chem. 7*, 258−280.

(18) Genin, M. J., Allwine, D. A., Anderson, D. J., et al. (2000) Substituent Effects on the Antibacterial Activity of Nitrogen-Carbon-Linked (Azolylphenyl)oxazolidinones with Expanded Activity Against the Fastidious Gram-Negative Organisms *Haemophilus influenzae* and *Moraxella catarrhalis*. *J. Med. Chem. 43*, 953−970.

(19) Louie, A., Liu, W., Kulawy, R., and Drusano, G. L. (2011) *In vivo* pharmacodynamics of torezolid phosphate (TR-701), a new oxazolidinone antibiotic, against methicillin-susceptible and methicillin-resistant *Staphyloccocus aureus* strains in a mouse thigh infection model. *Antimicrob. Agents Chemother. 55* (7), 3453−3460.

(20) Lepak, A. J., Marchillo, K., Pichereau, S., Craig, W. A., and Andes, D. R. (2012) Comparative pharmacodynamics of the new oxazolidinone tedizolid phosphate in a neutropenic murine *Staphyloccocus aureus* pneumonia model. *Antimicrob. Agents Chemother. 56* (11), 5916−5922.

(21) Renslo, A. R. (2010) Antibacterial oxazolidinones: emerging structure−toxicity relationships. *Expert Rev. Anti-Infect. Ther. 8* (5), 565−574.

(22) Reck, F., Zhou, F., Eyermann, C. J., et al. (2007) Novel substituted (pyridine-3-yl)phenyloxazolidinones: antibacterial agents with reduced activity against monoamine oxidase A and increased solubility. *J. Med. Chem. 50*, 4868−4881.

DOI: 10.1021/acsinfecdis.6b00003
ACS Infect. Dis. 2016, 2, 405−426

(23) Gerson, S. L., Kaplan, S. L., Bruss, J. B., et al. (2002) Hematologic effects of linezolid: summary of clinical experience. *Antimicrob. Agents Chemother. 46* (8), 2723−2726.
(24) Shaw, K. J., and Barbachyn, M. R. (2011) The oxazolidinones: past, present, and future. *Ann. N.Y. Acad. Sci. 1241*, 48−70.
(25) Woo, J. Y., Bin Im, W., Kaol Rhee, J., Ja Shim, M., Bae Kim, W., and Chil Choi, E. (2004) Synthesis and antibacterial activity of oxazolidinones containing pyridine substituted with heteroaromatic ring. *Bioorg. Med. Chem. 12*, 5909−5915.
(26) Wilson, D. N., Schluenzen, F., Harms, J. M., Starosta, A. L., Connell, S. R., and Fucini, P. (2008) The oxazolidinone antibiotics perturb the ribosomal peptidyl-transferase center and effect tRNA positioning. *Proc. Natl. Acad. Sci. U.S.A. 105* (36), 13339−13344.
(27) Gu, B., Kelesidis, T., Tsiaodras, S., et al. (2013) The emerging problem of linezolid-resistant *Staphylococcus*. *J. Antimicrob. Chemother. 68* (1), 4−11.
(28) Diaz, L., Kiratisin, P., Mendes, R. E., et al. (2012) Transferable plasmid-mediated resistance to linezolid due to cfr in a human clinical isolate of *Enterococcus faecalis*. *Antimicrob. Agents Chemother. 56* (7), 3917−3922.
(29) Mendes, R. E., Hogan, P. A., Streit, J. M., Jones, R. N., and Flamm, R. K. (2014) Zyvox® Annual Appraisal of Potency and Spectrum (ZAAPS) Program: report of linezolid activity over 9 years (2004−12). *J. Antimicrob. Chemother. 69*, 1582−1588.
(30) Locke, J. B., Finn, J., Hilgers, M., et al. (2010) Structure-activity relationships of diverse oxazolidinones for linezolid-resistant *Staphyloccocus aureus* strains possessing the *cfr*-methyltransferase gene or ribosomal mutations. *Antimicrob. Agents Chemother. 54* (12), 5337−5343.
(31) Lawrence, L., Danese, P., DeVito, J., et al. (2008) In vitro activity of Rx-01 oxazolidinones against hospital and community pathogens. *Antimicrob. Agents Chemother. 52* (5), 1653−1662.
(32) Schumacher, A., Trittler, R., Bohnert, J. A., et al. (2007) Intracellular accumulation of linezolid in *Escherichia coli*, *Citrobacter freundii,* and *Enterbacter aerogenes*: role of enhanced efflux pump activity and inactivation. *J. Antimicrob. Chemother. 59*, 1261−1264.
(33) Schaadt, R., Sweeney, D., Shinabarger, D., and Zurenko, D. (2009) In Vitro Activity of TR-700, the Active Ingredient of the Antibacterial Prodrug TR-701, a Novel Oxazolidinone Antibacterial Agent. *Antimicrob. Agents Chemother. 53*, 3236−3239.
(34) Ippolito, J. A., Kanyo, Z. F., Wang, D., Franceschi, F. J., Steitz, T. A., and Duffy, E. M. (2008) Crystal Structure of the Oxazolidinone Antibiotic Linezolid Bound to the 50S Ribosomal Subunit. *J. Med. Chem. 51*, 3353−3356.
(35) Zgurskaya, H. I., Krishnamoorthy, G., Ntreh, A., and Lu, S. (2011) Mechanism and Function of the Outer Membrane Channel TolC in Multidrug Resistance and Physiology of Enterobacteria. *Front. Microbiol. 2*, 00189.
(36) Clinical and Laboratory Standards Institute. (2014) *Performance Standards for Antimicrobial Susceptibility Testing, Twentieth Informational Supplement*, M100−S24, Clinical and Laboratory Standards Institute, Wayne, PA, USA.
(37) Sahalan, A. Z., and Dixon, R. A. (2008) Role of the cell envelope in the antibacterial activities of polymyxin B and polymyxin B nonapeptide against *Escherichia coli*. *Int. J. Antimicrob. Agents 31* (3), 224−227.
(38) Poole, K. (2000) Efflux-mediated resistance to fluoroquinolones in Gram-negative bacteria. *Antimicrob. Agents Chemother. 44* (9), 2233−2341. Singh, R., et al. (2012) Temporal interplay between efflux pumps and target mutations in development of antibiotic resistance in *Escherichia coli*. *Antimicrob. Agents Chemother. 56* (4), 1680−1685.

DOI: 10.1021/acsinfecdis.6b00003
ACS Infect. Dis. 2016, 2, 405−426